CHARACTERIZING THE INTERACTIONS OF TROPOMYOSIN RECEPTOR KINASES (TRKS) IN THE PLASMA MEMBRANE

by
Fozia Ahmed

A dissertation submitted to Johns Hopkins University in conformity with the requirements for the degree of Doctor of Philosophy

Baltimore, Maryland
March, 2019

Abstract

The three Tropomyosin Receptor Kinases, Trk-A, Trk-B, and Trk-C, belong to the second largest class of membrane proteins, the Receptor Tyrosine Kinases (RTKs). The Trks are important for the survival and the function of neurons in the central nervous system, and have been implicated in many cancers. Currently, the Trks are known to bind neurotrophins and get activated upon lateral dimerization, but there is no quantitative or mechanistic understanding of the dimerization process. This is one bottleneck in the development of Trk targeted therapies. The goal of this project is to characterize the interactions that control Trk activation in the plasma membrane using a FRET-based method.

To determine the propensity for Trk dimerization in quantitative terms, I have characterized the dimerization of each Trk receptor over a broad range of concentrations in live cells. This has been done in the absence and in the presence of their ligands, the neurotrophins. I have found that the Trk receptors form dimers even in the absence of ligands, stabilized mainly via contacts in the transmembrane/intracellular domains, and binding of their cognate ligands stabilizes the dimers and induces changes in the conformations of the kinase dimers.

I have also explored the mechanism of ligand functional selectivity for Trk-A and Trk-B. Ligand functional selectivity, or ligand biased signaling, is a phenomenon in which different ligands lead to different biological outcomes while interacting with the same receptor. I have shown that different ligand-bound Trk-A dimers have different stabilities, and that different ligand-bound Trk-B dimers exhibit both different stabilities and different intracellular conformations. These differences likely underlie the differential signaling in response to the different ligands.

In the long run, this new basic knowledge about Trk interactions in the absence and presence of ligands may be used for the design of targeted Trk inhibitors, for the benefit of human health.

Readers

Professor Kalina Hristova (Advisor)

Professor Luo Gu

Acknowledgements

I would like to express my special thanks of gratitude to my wonderful advisor Professor Kalina Hristova for providing me with the opportunity to work on this exciting project and also with amazing group of people. In research, you have always supported my ideas and provided me with positive feedback to promote my curiosity. I have learned from you that every experiment regardless of the results is invaluable. Also, I am grateful for the fact that you have always supported activities outside research which were essential for my professional career growth. Thank you for all your support and encouragement, and making my Ph.D journey very dynamic and fascinating. I am very lucky to have you as my advisor.

A very special thanks to my lab fellows and wonderful friend Nuala Del Piccolo and Michael Paul, who have always shown willingness to discuss ideas, brain storm and trouble shoot experiments. You have shown immense patience in discussing every scientific theory/idea I had. I really appreciate your support.

Also, I am thankful to all the magnificent people in Hristova lab: Sarah Kim, Alexander Komin, Elmer Zapata Mercado, Taylor Light, Sewwandi Rathnayake, Kelly Karl, and Daniel Wirth. Thank you for providing me with the wonderful productive lab environment to work and strong support system. Special thanks to Sarah Kim and Alexander Komin for long discussions about our careers and opportunities available for career development at and around Johns Hopkins.

My Mamma and Pappa, my older brother, Amjad Ali, best friend, Kalpana Besar, and my husband, Mirza Saad Ahmed; thank you for your unconditional love and constant support, and having faith in my capabilities for all these years.

Finally, I would like to thank my Thesis Defense Committee: Dr. Stavroula Sofou,

Dr. Feilim Mac Gabhann, Dr. Jamie Spangler, and Dr. Luo Gu for their time and valuable advice.

Note: Additional acknowledgements for each projects will be stated at the end of each chapter.

Table of Contents

List of Figures

List of Tables

Chapter 1: Introduction

1-1: Membrane Proteins

The sequenced human genome has shown that membrane proteins account for 30% of all the proteins. However, only 2% of these protein structures are deposited in the protein data bank, and thus very few high-resolution structures are available [1]. This is due to inherent limitations that the researchers face when working with membrane proteins in order to crystalize them [2][3]. There is a strong need to overcome these challenges or to discover alternative study methodologies since membrane proteins represent 60% of drug targets being explored for various therapies, due to their crucial role in initiating signaling pathways [4][5].

1-2: Protein-Protein Interactions

The membrane proteins are embedded in the cell's plasma membrane, where they control incoming messages to the cells by various mechanisms. One mechanism by which these proteins control signaling is via protein-protein interaction in the membrane. Protein-protein interactions in plasma membranes play important role in regulating the transmission of signals from the external environment to the cell cytoplasm. These proteins initiate signaling through various downstream pathways and control biological responses such as cell growth, survival, differentiation, and migration, and thus are under study for targeted drug discovery [6][7][8][9] [10][11].

1-3: Receptor Tyrosine Kinases (RTKs)

Receptor Tyrosine Kinases (RTKs) are one class of membrane proteins and of interest to scientific research due to their diversity in activation and their significant role in diseases like cancers, diabetes, inflammatory disorders, and bone disorders. These disorders occur due to

dysregulation caused by genetic alterations or other factors and lead to abnormal signaling [8], [11]. New drugs are being developed to either block or alter RTKs activity in diseases. In terms of their structure, these membrane receptors contain an extracellular (EC) domain, where ligand binds, a transmembrane domain (TM), which goes through the plasma membrane, and a tyrosine kinase domain (TK), which is present in the intracellular region; they also contain carboxy terminal and juxtamembrane regions [8] . RTKs share similarities in their structure, but the responses elicited by each RTK can be very different as they regulate highly specific pathways involved in distinctive cellular responses. Thus far, 58 RTKs have been identified belonging to 20 subfamilies in humans, based on the molecular characteristics of their extracellular domains [12].

For RTK activation, in general, the binding of ligand to the receptor initiates downstream signaling [11][13][14]. Currently, there are two competing models proposed for RTK interaction and activation in the plasma membrane as shown in Figure 1-1. Figure 1-1-A is a representation of the canonical model or "diffusion-based" model, where two monomers present in the plasma membrane come in close proximity in the presence of ligand. As a result, dimerization occurs. The tyrosine kinase domains get activated, and initiate biological signaling by recruiting downstream molecules (adaptors) to the phosphorylated sites of the receptors. The adaptors are phosphorylated by the RTKs and initiate biological responses [15][16]. Figure 1-1-B is a representation of a model known as the "pre-formed dimer model". In this model, pre-formed dimers exist in the absence of ligands. Upon ligand binding these dimers are stabilized. Furthermore, there is a change in the conformation of the dimers, leading to the activation of the kinase domains to initiate downstream signaling as mentioned above [17][18]. The unliganded

dimers have been shown to have basal level phosphorylation activity and are associated with the progression of various disorders and cancers [8][19][20].

These two models for RTK interaction and activation differ due to the absence or presence of unliganded RTK dimers. In this thesis, I investigate which of the RTK activation model is applicable to one subfamily of RTK receptors, the Tropomyosin receptor kinases (Trks).

1-4: Tropomyosin Receptor Kinases (Trks)

The subfamily of Tropomyosin receptor kinases (Trks) consists of three members: Tropomyosin receptor kinase-A, B, and C. The Trks extracellular domains consist of leucine rich repeats (LRR) flanked by two cysteine clusters, followed by two immunoglobulin like domains (Ig1 and Ig2) as shown in figure 1-2 [21]. The three Trk receptors are highly similar in terms of their structure. The protein sequence percent homology for Trk-A and Trk-B is 49%, for Trk-A and Trk-C it is 51%, and for Trk-B and Trk-C it is 55%. The kinase domain sequence percent homology for all three Trks are 71% [22][23]. Despite very similar structures, these Trks play distinct roles in the development of the central nervous system. Trk-A is important for the development of normal sympathetic neurons, Trk-B is responsible for proper development of sensory neurons, and Trk-C has overlapping role with Trk-A during sympathetic neuron development. Trk-C is present during early stages of development while Trk-A predominates during later stages of the development of sympathetic neurons [24][25][26][27][28][29].

The Trk receptors are activated by four ligands, called neurotrophins: Nerve Growth Factor (NGF), Neurotrophin -3 (NT-3), Neurotrophin-4 (NT-4) and brain-derived neurotrophic factor (BDNF) [30], [31], [32], [33]. The Trks play diverse roles in the development of the mammalian nervous system by promoting survival and differentiation of neurons in the presence

of neurotrophins [34]. They control synaptic strength, plasticity, neuronal survival, proliferation, migration, axonal growth/guidance and patterning, injury protection, and neuronal apoptosis [32][33][35][36][37][38][30][39]. Trks have been shown to be involved in pain sensation malignancy and in tumor growth and survival [22][40]. Trk-A has been associated with papillary thyroid, colon cancer, neuroblastoma, and lung cancers [22][41][42][43], and also with congenital insensitivity to pain with anhidrosis (CIPA)[44][45]. Trk-B has been reported to be involved in metastatic stages and in aggressive tumor growth in human pancreatic cancer and neuroblastoma [46], [47]. Trk-C has been involved in secretory breast carcinoma and in acute myeloid leukemias (AML)[48].

There are multiple mechanisms responsible for the involvement of Trks in diseases and cancers. CIPA has been associated with point mutations in Trks. Chimeric oncogenes which are created by chromosomal rearrangement are involved in the transformation, proliferation, and survival of cancer cells. In these chimeric exchanges, the extracellular domain belongs to different genes while the TM and TK domains are from a Trk receptor [49]. Gene deletions and splice variations leading to loss of the extracellular region have also been shown to be associated with AML and neuroblastomas [21].This linkage of the Trk family to cancers and CIPA has promoted a significant interest in the development of targeted therapies for Trk associated malignancies. However, development of successful Trk inhibitors is still a challenge. One of the main reasons for the current low success rate for Trk targeted therapies is the incomplete understanding of Trks activation and interactions in the plasma membrane. This lack of basic knowledge about Trk function is a bottleneck for the development of specific therapies.

1-5: Ligand Biased Signaling for Trk-A and Trk-B

Tropomyosin receptor kinase-A and B are also involved in ligand-biased signaling, in which one receptor responds to multiple ligands to initiate ligand-specific downstream biological responses. Trk-A not only interacts with its cognate ligand hß-NGF but it also interacts with h-NT-3, which is a cognate ligand for Trk-C. When Trk-A interacts with hß-NGF, Trk-A activation initiates signaling cascades which promote survival of neurons. In the presence of h-NT-3, Trk-A activates a pathway which is involved in axon extension of neurons [50]. Therefore, hß-NGF and h-NT-3 differentially regulate the same Trk-A receptor, leading to selective biological responses. Trk-B interacts with h-NT-3 and h-NT-4, besides its cognate ligand h-BDNF. In the presence of h-BDNF, Trk-B generates responses which promote synaptic transmission and plasticity [51][52][53]. In the presence of h-NT-4, Trk-B supports the survival of neurons and synaptic maturation [54][54][55][56]. In the presence of h-NT-3, Trk-B mainly initiates signaling to promote the survival of Trk-B expressing neurons [57][51][52][58][59][60][61].

There are two existing hypotheses about this phenomenon in which different ligands generate different responses via the same receptor. One hypothesis is that each ligand induces different structural changes in the extracellular domain of the receptor, and then these changes are transmitted to the kinase domains via the transmembrane region, causing the kinase dimer configuration to change. This leads to site-specific phosphorylation and recruitment of different downstream signaling molecules [62]. The second hypothesis focuses on changes in dimer stability in the presence of different ligands [63]. There are no studies which have investigated these two hypotheses for the Trk receptors, and the interactions and activation of Trk-A and Trk-B with different ligands have not been compared. My work will explore these hypotheses in

terms of Trk receptor ligand-biased signaling. Receptor interactions in the plasma membrane will be investigated using a Förster Resonance Energy Transfer (FRET)-based method. The methodology utilizes fluorophores attached to a receptor to directly quantify the interactions as described in detail in chapter 2.

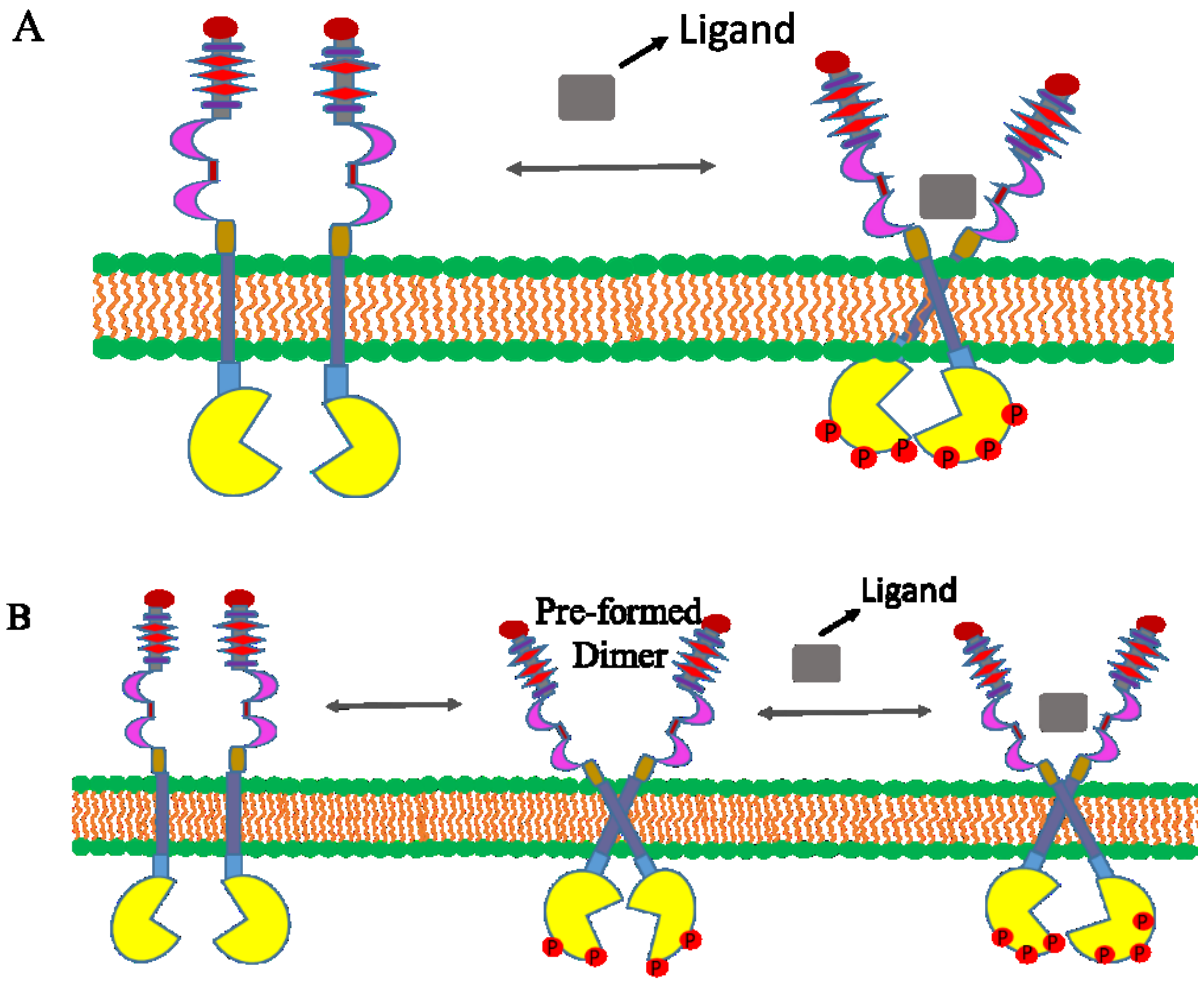

Figure 1- 1: Representation of the canonical or "diffusion-based" and the "pre-formed dimer" models of RTK activation.

A) Representation of the canonical model for RTK activation. This model assumes that RTKs exist as monomers in the plasma membrane in the absence of ligands. Upon ligand binding, these monomers dimerize and cross-phosphorylate their kinase domains to activate them. B) Representation of a new emerging model for RTK activation known as the pre-formed dimer model. In this model, RTKs exist as monomers and dimers in the absence of ligands. Upon ligand binding these preformed dimers undergo structural and stability changes to start downstream signaling.

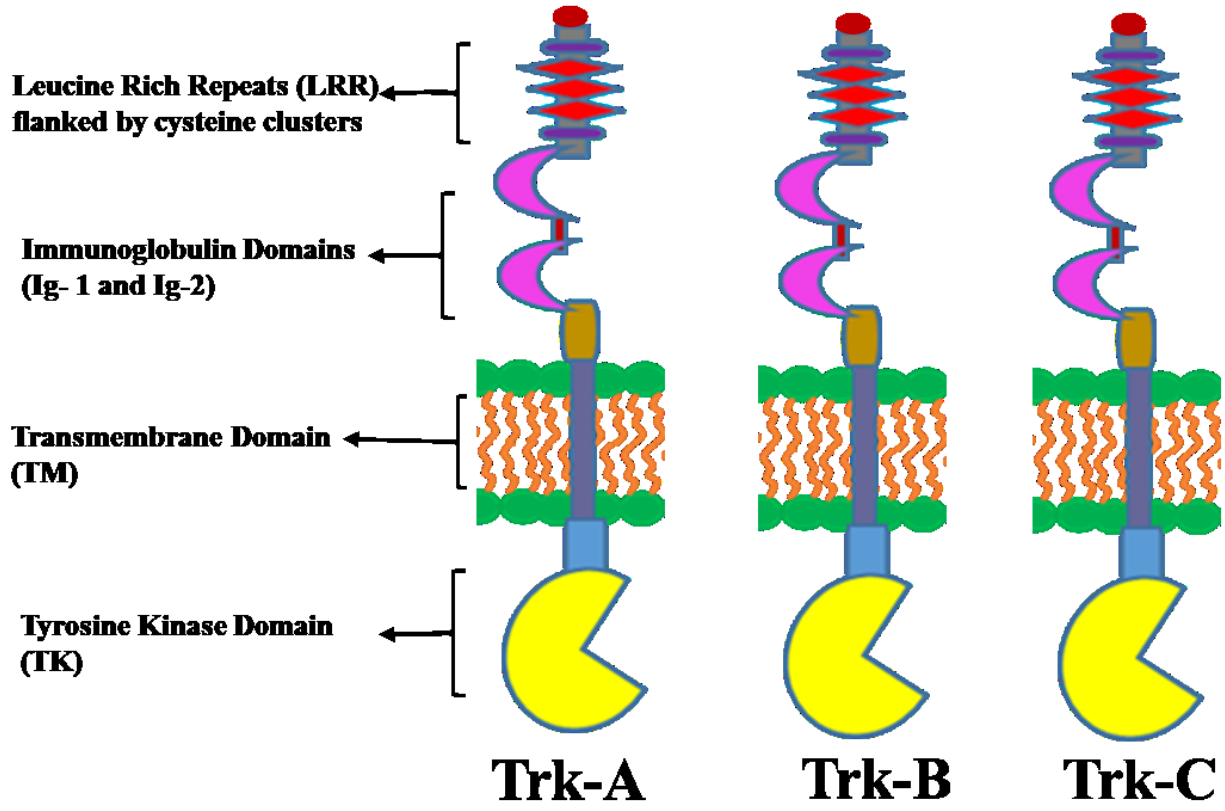

Figure 1- 2: Structural details of the Trk-A, B, and C receptors. The extracellular regions consist of leucine rich repeats, which are flanked by cysteine clusters, and two immunoglobulin domains (Ig-1 and Ig-2). A single pass transmembrane region spans the plasma membranes and is followed by an intracellular kinase domain.

1-6: References

[1] Y. Arinaminpathy, E. Khurana, D. M. Engelman, and M. B. Gerstein, "Computational analysis of membrane proteins: the largest class of drug targets.," *Drug Discov. Today*, vol. 14, no. 23–24, pp. 1130–5, Dec. 2009.

[2] J. N. Sachs and D. M. Engelman, "Introduction to the membrane protein reviews: the interplay of structure, dynamics, and environment in membrane protein function.," *Annu. Rev. Biochem.*, vol. 75, pp. 707–12, 2006.

[3] R. Grisshammer and C. G. Tate, "Overexpression of integral membrane proteins for structural studies.," *Q. Rev. Biophys.*, vol. 28, no. 3, pp. 315–422, Aug. 1995.

[4] G. C. Terstappen and A. Reggiani, "In silico research in drug discovery.," *Trends Pharmacol. Sci.*, vol. 22, no. 1, pp. 23–6, Jan. 2001.

[5] J. Davey, "G-protein-coupled receptors: new approaches to maximise the impact of GPCRS in drug discovery.," *Expert Opin. Ther. Targets*, vol. 8, no. 2, pp. 165–70, Apr. 2004.

[6] A. Wells, "EGF receptor.," *Int. J. Biochem. Cell Biol.*, vol. 31, no. 6, pp. 637–43, Jun. 1999.

[7] B. Linggi and G. Carpenter, "ErbB receptors: new insights on mechanisms and biology.," *Trends Cell Biol.*, vol. 16, no. 12, pp. 649–56, Dec. 2006.

[8] M. A. Lemmon and J. Schlessinger, "Cell signaling by receptor tyrosine kinases.," *Cell*, vol. 141, no. 7, pp. 1117–34, Jun. 2010.

[9] J. P. Overington, B. Al-Lazikani, and A. L. Hopkins, "How many drug targets are there?," *Nat. Rev. Drug Discov.*, vol. 5, no. 12, pp. 993–6, Dec. 2006.

[10] P. Blume-Jensen and T. Hunter, "Oncogenic kinase signalling.," *Nature*, vol. 411, no.

6835, pp. 355–65, May 2001.

[11] A. Ullrich and J. Schlessinger, “Signal transduction by receptors with tyrosine kinase activity.,” *Cell*, vol. 61, no. 2, pp. 203–12, Apr. 1990.

[12] A. I. Ségaliny, M. Tellez-Gabriel, M.-F. Heymann, and D. Heymann, “Receptor tyrosine kinases: Characterisation, mechanism of action and therapeutic interests for bone cancers.,” *J. bone Oncol.*, vol. 4, no. 1, pp. 1–12, Mar. 2015.

[13] W. A. Barton *et al.*, “Crystal structures of the Tie2 receptor ectodomain and the angiopoietin-2-Tie2 complex.,” *Nat. Struct. Mol. Biol.*, vol. 13, no. 6, pp. 524–32, Jun. 2006.

[14] J.-P. Himanen and D. B. Nikolov, “Eph signaling: a structural view.,” *Trends Neurosci.*, vol. 26, no. 1, pp. 46–51, Jan. 2003.

[15] J. Schlessinger, “Cell Signaling by Receptor Tyrosine Kinases,” *Cell*, vol. 103, no. 2, pp. 211–225, Oct. 2000.

[16] J. Schlessinger, “Receptor tyrosine kinases: legacy of the first two decades.,” *Cold Spring Harb. Perspect. Biol.*, vol. 6, no. 3, Mar. 2014.

[17] S. Sarabipour, K. Ballmer-Hofer, and K. Hristova, “VEGFR-2 conformational switch in response to ligand binding.,” *Elife*, vol. 5, p. e13876, Apr. 2016.

[18] S. Sarabipour and K. Hristova, “Mechanism of FGF receptor dimerization and activation.,” *Nat. Commun.*, vol. 7, p. 10262, Jan. 2016.

[19] M. A. Lemmon, J. Schlessinger, and K. M. Ferguson, “The EGFR family: not so prototypical receptor tyrosine kinases.,” *Cold Spring Harb. Perspect. Biol.*, vol. 6, no. 4, p. a020768, Apr. 2014.

[20] N. E. Hynes and H. A. Lane, “ERBB receptors and cancer: the complexity of targeted

inhibitors.," *Nat. Rev. Cancer*, vol. 5, no. 5, pp. 341–54, May 2005.

[21] J. C. Arevalo, B. Conde, B. L. Hempstead, M. V Chao, D. Martin-Zanca, and P. Perez, "TrkA immunoglobulin-like ligand binding domains inhibit spontaneous activation of the receptor.," *Mol. Cell. Biol.*, vol. 20, no. 16, pp. 5908–16, Aug. 2000.

[22] A. Nakagawara, "Trk receptor tyrosine kinases: a bridge between cancer and neural development.," *Cancer Lett.*, vol. 169, no. 2, pp. 107–14, Aug. 2001.

[23] A. Nakagawara *et al.*, "Cloning and chromosomal localization of the human TRK-B tyrosine kinase receptor gene (NTRK2).," *Genomics*, vol. 25, no. 2, pp. 538–46, Jan. 1995.

[24] M. Barbacid, "Structural and functional properties of the TRK family of neurotrophin receptors.," *Ann. N. Y. Acad. Sci.*, vol. 766, pp. 442–58, Sep. 1995.

[25] A. M. Fagan, H. Zhang, S. Landis, R. J. Smeyne, I. Silos-Santiago, and M. Barbacid, "TrkA, but not TrkC, receptors are essential for survival of sympathetic neurons in vivo.," *J. Neurosci.*, vol. 16, no. 19, pp. 6208–18, Oct. 1996.

[26] R. Levi-Montalcini, "The nerve growth factor 35 years later.," *Science*, vol. 237, no. 4819, pp. 1154–62, Sep. 1987.

[27] L. G. Piñon, L. Minichiello, R. Klein, and A. M. Davies, "Timing of neuronal death in trkA, trkB and trkC mutant embryos reveals developmental changes in sensory neuron dependence on Trk signalling.," *Development*, vol. 122, no. 10, pp. 3255–61, Oct. 1996.

[28] J. E. Dixon and D. McKinnon, "Expression of the trk gene family of neurotrophin receptors in prevertebral sympathetic ganglia.," *Brain Res. Dev. Brain Res.*, vol. 77, no. 2, pp. 177–82, Feb. 1994.

[29] A. Schober *et al.*, "Reduced acetylcholinesterase (AChE) activity in adrenal medulla and

loss of sympathetic preganglionic neurons in TrkA-deficient, but not TrkB-deficient, mice.," *J. Neurosci.*, vol. 17, no. 3, pp. 891–903, Feb. 1997.

[30] D. R. Kaplan and F. D. Miller, "Neurotrophin signal transduction in the nervous system.," *Curr. Opin. Neurobiol.*, vol. 10, no. 3, pp. 381–91, Jun. 2000.

[31] F. Lamballe, R. Klein, and M. Barbacid, "trkC, a new member of the trk family of tyrosine protein kinases, is a receptor for neurotrophin-3.," *Cell*, vol. 66, no. 5, pp. 967–79, Sep. 1991.

[32] E. J. Huang and L. F. Reichardt, "Neurotrophins: roles in neuronal development and function.," *Annu. Rev. Neurosci.*, vol. 24, pp. 677–736, 2001.

[33] M. Bibel and Y. A. Barde, "Neurotrophins: key regulators of cell fate and cell shape in the vertebrate nervous system.," *Genes Dev.*, vol. 14, no. 23, pp. 2919–37, Dec. 2000.

[34] G. M. Brodeur *et al.*, "Trk receptor expression and inhibition in neuroblastomas.," *Clin. Cancer Res.*, vol. 15, no. 10, pp. 3244–50, May 2009.

[35] J. R. Chan, J. M. Cosgaya, Y. J. Wu, and E. M. Shooter, "Neurotrophins are key mediators of the myelination program in the peripheral nervous system.," *Proc. Natl. Acad. Sci. U. S. A.*, vol. 98, no. 25, pp. 14661–8, Dec. 2001.

[36] B. L. Hempstead and J. L. Salzer, "Neurobiology. A glial spin on neurotrophins.," *Science*, vol. 298, no. 5596, pp. 1184–6, Nov. 2002.

[37] A. Patapoutian and L. F. Reichardt, "Trk receptors: mediators of neurotrophin action.," *Curr. Opin. Neurobiol.*, vol. 11, no. 3, pp. 272–80, Jun. 2001.

[38] M. V Sofroniew, C. L. Howe, and W. C. Mobley, "Nerve growth factor signaling, neuroprotection, and neural repair.," *Annu. Rev. Neurosci.*, vol. 24, pp. 1217–81, 2001.

[39] F. D. Miller and D. R. Kaplan, "Neurobiology. TRK makes the retrograde.," *Science*, vol.

295, no. 5559, pp. 1471–3, Feb. 2002.

[40] C. J. Desmet and D. S. Peeper, “The neurotrophic receptor TrkB: a drug target in anti-cancer therapy?,” *Cell. Mol. Life Sci.*, vol. 63, no. 7–8, pp. 755–9, Apr. 2006.

[41] A. Tacconelli *et al.*, “TrkA alternative splicing: a regulated tumor-promoting switch in human neuroblastoma.,” *Cancer Cell*, vol. 6, no. 4, pp. 347–60, Oct. 2004.

[42] A. Bardelli *et al.*, “Mutational analysis of the tyrosine kinome in colorectal cancers.,” *Science*, vol. 300, no. 5621, p. 949, May 2003.

[43] A. M. Davies, K. F. Lee, and R. Jaenisch, “p75-deficient trigeminal sensory neurons have an altered response to NGF but not to other neurotrophins.,” *Neuron*, vol. 11, no. 4, pp. 565–74, Oct. 1993.

[44] Y. Indo *et al.*, “Congenital insensitivity to pain with anhidrosis (CIPA): novel mutations of the TRKA (NTRK1) gene, a putative uniparental disomy, and a linkage of the mutant TRKA and PKLR genes in a family with CIPA and pyruvate kinase deficiency.,” *Hum. Mutat.*, vol. 18, no. 4, pp. 308–18, Oct. 2001.

[45] Y. Indo *et al.*, “Mutations in the TRKA/NGF receptor gene in patients with congenital insensitivity to pain with anhidrosis.,” *Nat. Genet.*, vol. 13, no. 4, pp. 485–8, Aug. 1996.

[46] G. M. Sclabas *et al.*, “Overexpression of tropomysin-related kinase B in metastatic human pancreatic cancer cells.,” *Clin. Cancer Res.*, vol. 11, no. 2 Pt 1, pp. 440–9, Jan. 2005.

[47] R. Ho *et al.*, “Resistance to chemotherapy mediated by TrkB in neuroblastomas.,” *Cancer Res.*, vol. 62, no. 22, pp. 6462–6, Nov. 2002.

[48] C. Tognon *et al.*, “Expression of the ETV6-NTRK3 gene fusion as a primary event in human secretory breast carcinoma.,” *Cancer Cell*, vol. 2, no. 5, pp. 367–76, Nov. 2002.

[49] A. Vaishnavi *et al.*, “Oncogenic and drug-sensitive NTRK1 rearrangements in lung

cancer.," *Nat. Med.*, vol. 19, no. 11, pp. 1469–1472, Nov. 2013.

[50] A. W. Harrington *et al.*, "Recruitment of actin modifiers to TrkA endosomes governs retrograde NGF signaling and survival.," *Cell*, vol. 146, no. 3, pp. 421–34, Aug. 2011.

[51] D. J. Glass *et al.*, "TrkB mediates BDNF/NT-3-dependent survival and proliferation in fibroblasts lacking the low affinity NGF receptor.," *Cell*, vol. 66, no. 2, pp. 405–13, Jul. 1991.

[52] D. Soppet *et al.*, "The neurotrophic factors brain-derived neurotrophic factor and neurotrophin-3 are ligands for the trkB tyrosine kinase receptor.," *Cell*, vol. 65, no. 5, pp. 895–903, May 1991.

[53] J. Hall, K. L. Thomas, and B. J. Everitt, "Rapid and selective induction of BDNF expression in the hippocampus during contextual learning.," *Nat. Neurosci.*, vol. 3, no. 6, pp. 533–5, Jun. 2000.

[54] N. Y. Ip *et al.*, "Similarities and differences in the way neurotrophins interact with the Trk receptors in neuronal and nonneuronal cells.," *Neuron*, vol. 10, no. 2, pp. 137–49, Feb. 1993.

[55] R. Klein, F. Lamballe, S. Bryant, and M. Barbacid, "The trkB tyrosine protein kinase is a receptor for neurotrophin-4.," *Neuron*, vol. 8, no. 5, pp. 947–56, May 1992.

[56] G. Fan *et al.*, "Knocking the NT4 gene into the BDNF locus rescues BDNF deficient mice and reveals distinct NT4 and BDNF activities.," *Nat. Neurosci.*, vol. 3, no. 4, pp. 350–7, Apr. 2000.

[57] C. Cordon-Cardo *et al.*, "The trk tyrosine protein kinase mediates the mitogenic properties of nerve growth factor and neurotrophin-3.," *Cell*, vol. 66, no. 1, pp. 173–83, Jul. 1991.

[58] J. Philo, J. Talvenheimo, J. Wen, R. Rosenfeld, A. Welcher, and T. Arakawa,

"Interactions of neurotrophin-3 (NT-3), brain-derived neurotrophic factor (BDNF), and the NT-3.BDNF heterodimer with the extracellular domains of the TrkB and TrkC receptors.," *J. Biol. Chem.*, vol. 269, no. 45, pp. 27840–6, Nov. 1994.

[59] A. Hohn, J. Leibrock, K. Bailey, and Y. A. Barde, "Identification and characterization of a novel member of the nerve growth factor/brain-derived neurotrophic factor family.," *Nature*, vol. 344, no. 6264, pp. 339–41, Mar. 1990.

[60] P. C. Maisonpierre *et al.*, "NT-3, BDNF, and NGF in the developing rat nervous system: parallel as well as reciprocal patterns of expression.," *Neuron*, vol. 5, no. 4, pp. 501–9, Oct. 1990.

[61] A. Rosenthal *et al.*, "Primary structure and biological activity of a novel human neurotrophic factor.," *Neuron*, vol. 4, no. 5, pp. 767–73, May 1990.

[62] R. A. Scheck, M. A. Lowder, J. S. Appelbaum, and A. Schepartz, "Bipartite tetracysteine display reveals allosteric control of ligand-specific EGFR activation.," *ACS Chem. Biol.*, vol. 7, no. 8, pp. 1367–76, Aug. 2012.

[63] D. M. Freed *et al.*, "EGFR Ligands Differentially Stabilize Receptor Dimers to Specify Signaling Kinetics.," *Cell*, vol. 171, no. 3, p. 683–695.e18, Oct. 2017.

Chapter 2: Experimental Materials and Methods

The experimental methods utilized in all the chapters are similar. The details about the materials utilized, the molecular cloning techniques used to generate recombinant Trk receptors, the cell culture and transfection protocols, the crosslinking protocol, the FRET image acquisition equipment, and the FRET image analysis are described in detail in this chapter.

2-1: Trk-A, Trk-B and Trk-C Plasmids Cloning

The pCMV5 Trk-A plasmid [1] was purchased from Addgene (# 15002). The Trk-A gene was amplified and cloned using the restriction enzyme method into a pcDNA3.1+ vector that has been previously engineered to incorporate a gene encoding for a 15 amino acid flexible $(GGS)_5$ linker followed by either eYFP or mTurquoise (a FRET pair)[2]. The ECTM-Trk-A plasmids, encoding for the Trk-A extracellular (EC) and transmembrane (TM) domains, a $(GGS)_5$ linker, and either eYFP or mTurquoise, were similarly generated. The TM-Trk-A plasmids, containing the transmembrane (TM) domains, a $(GGS)_5$ linker, and either eYFP or mTurquoise, were produced via Gibson assembly using the NEBuilder HiFi DNA assembly kit (New England Biolabs, E5520S), following the manufacturer's protocols.

The pDNR-Dual Trk-B plasmid (# HsCD00022371) and pDNR-Dual Trk-C plasmid (# HsCD00022362) were purchased from the DNASU Plasmid Repository. Trk-B and Trk-C, and their ECTM and TM versions were cloned into the pcDNA 3.1+ vector, which incorporated the $(GGS)_5$ linker and the fluorescent protein (either eYFP or mTurquoiuse). Cloning was performed via Gibson assembly using the NEBuilder HiFi DNA assembly kit (New England Biolabs, E5520S). All plasmid constructs are shown in Figure 2-1. The primer design for all the constructs is shown in Table 2-1. The schematic of the Trk receptors is shown in Figure 2-2.

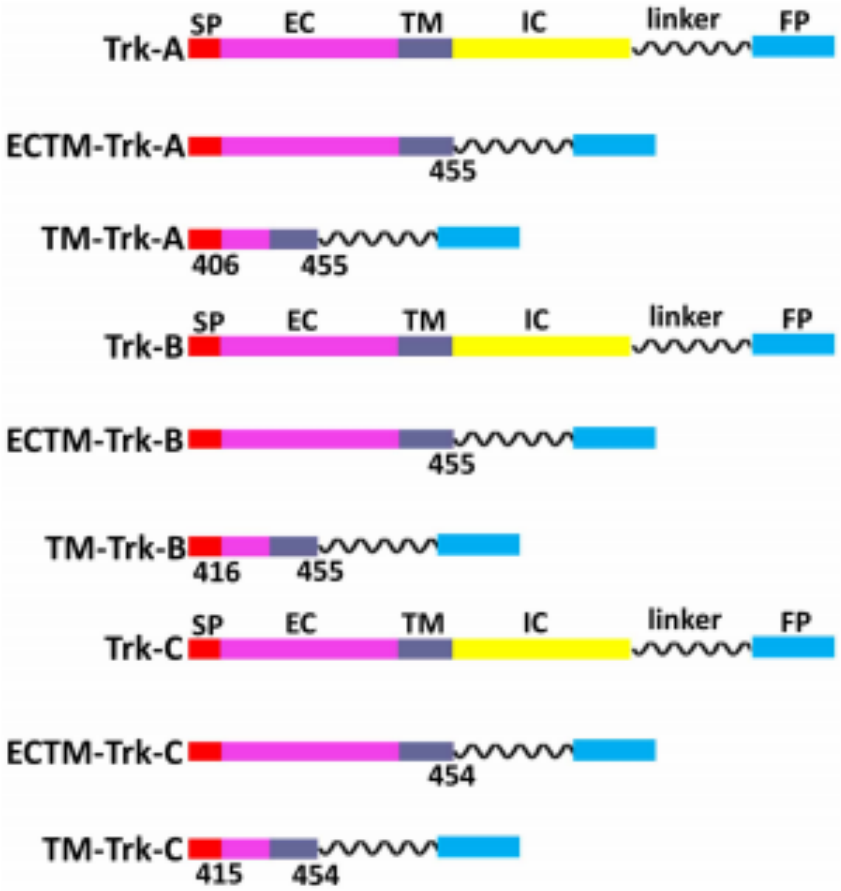

Figure 2- 1: Schematics of Trk-A, B, and C constructs, cloned for the FRET experiments. The numbers below the constructs indicate where the DNA sequence was cut to create the truncated constructs.

Receptor primers	Primer Sequences
FW Trk-A	5' –GCC AAG CTT GCC ACC ATG CTG CGA GGC GG– 3'
RV Trk-A	5' –GTC TAC CTG GAT GTC CTG GGC GAA TTC GCC GCC GCC– 3'
RV ECTM-Trk-A	5' –GGC GGC GGC GAA TTC TCT CCG TCC ACA TTT GTT GAGC– 3'
FW SP-Trk-A	5' –ATCTGCGGGCGACCCGGTGGAGAAGAAGGAC– 3'
RV SP-Trk-A	5' –GGTGGCAAGCTTAAGTTTAAAC– 3'
FW TM-Trk-A	5' –GATATCGGAGGAAGTGGCGG– 3'
RV TM-Trk-A	5' –CCACCGGGTCGCCCGCAGATGCCAGTATCAGCC– 3'
FW pcDNA-TM-A	5' –TTAAACTTAAGCTTGCCACCATGCTGCGAGGCGGACGGCG– 3'
RV pcDNA-TM-A	5' –CCGCCACTTCCTCCGATATCTCTCCGTCCACATTTGTTGAGC– 3'
FW Trk-B	5' –TTAAACTTAAGCTTGCCACCATGTCGTCCTGGATAAGGTG– 3'
RV Trk-B	5' –CCGCCACTTCCTCCGATATCGCCTAGAATGTCCAGGTAGAC– 3'
FW ECTM-Trk-B	5'–TTAAACTTAAGCTTGCCACCATGTCGTCCTGGATAAGGTG– 3'
RV ECTM-Trk-B	5'–CCGCCACTTCCTCCGATATCCTTAAGCAGAAACAGCATTACC– 3'
FW Trk-C	5'–GCCAAGCTTGCCACCATGGATGTCTCTCTTTGCCCAGCC –3'
RV Trk-C	5'–GGCGGCGGCGATATC G C CAAGAATGT CCAGGTAGATT–3'
RV ECTM-Trk-C	5'–GGCGGCGGCGATATCGTTGATCATGACGAAGAGAACCAC–5'

Table 2- 1: Primers used to clone Trk-A, B, and C and their truncated versions. FW: forward primer; RV: reverse primer; SP: signal peptide; TM: transmembrane domain, ECTM: extracellular + transmembrane domains.

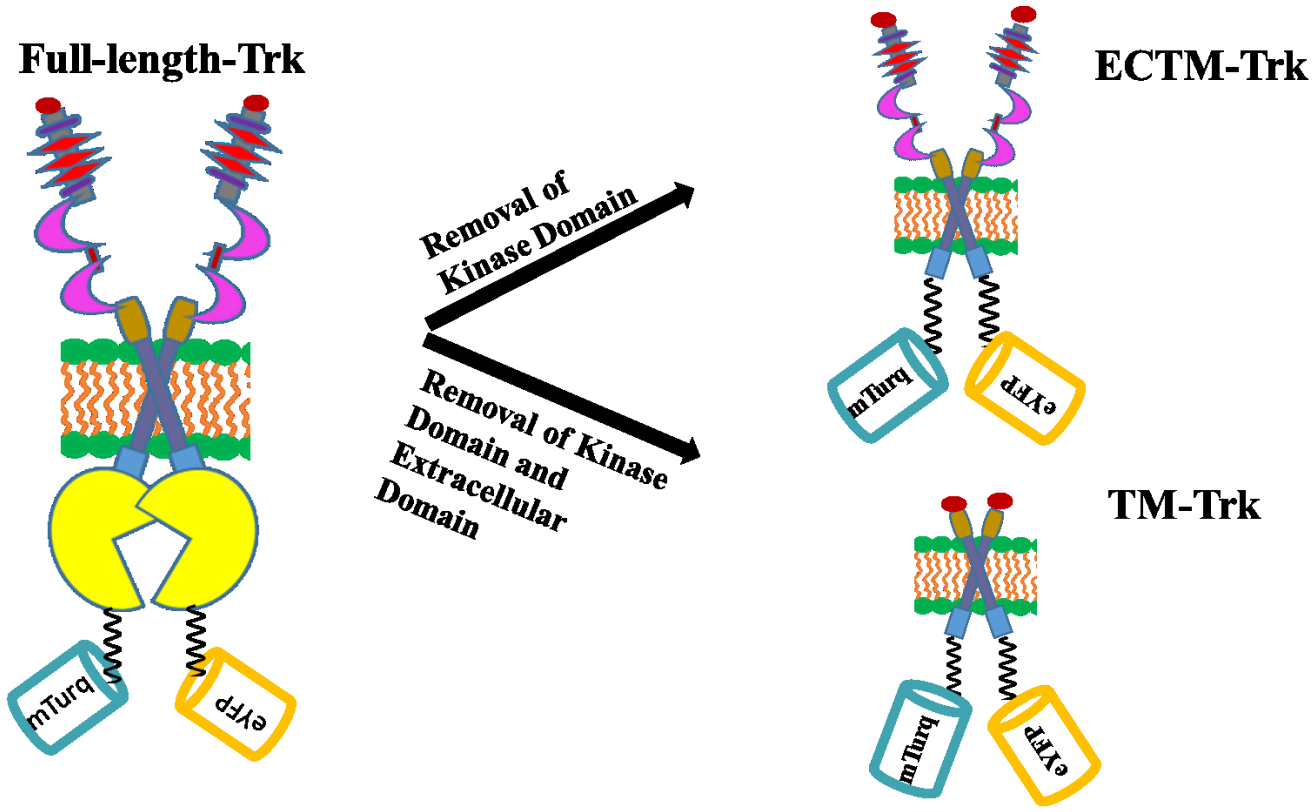

Figure 2- 2: The schematics of full length Trk receptor, Extracellular Transmembrane Trk receptor (ECTM-Trk), and Transmembrane Trk receptor (TM-Trk) attached to the fluorophores mTurquoise (donor) and eYFP (acceptor) via a 15 amino acid flexible linker.

2-2: Cell Culture and Transfection

Human embryonic kidney cells (HEK293T) used in this work were a kind gift from Dr. D. Wirtz, Johns Hopkins University. The cells were cultured in Dublecco's Modified Eagle Medium (DMEM, ThermoFisher Scientific, 31600034) with 10% fetal bovine serum (FBS, Hylone, SH30070.03), at 37^0C in the presence of 5% CO_2.

To perform the FRET experiments, HEK293T cells were seeded (2.5 X 10^5 cells/dish) on collagen coated, glass bottom petri dishes (MatTek, P35GCOL-1.5-14-C). Upon reaching 60% confluency, cells were transfected with 2ug of DNA using Fugene HD (Promega, E2311) according to the manufacturer's protocol. In the FRET experiments, cells were co-transfected with different ratios of Trk-mTurquoise and Trk-eYFP DNA. Control single transfection experiments were also conducted, where cells were singly transfected with either Trk-mTurquoise or Trk-eYFP DNA; the acquired spectra were used for calibration as previously described [3]. Twenty four hours post transfection, cells were rinsed twice with phenol-red and serum free medium, and starved in the same media for 12 hours. In some experiments, the ligands human ß-nerve growth factor (hß-NGF, Cell Signaling Technology, 5221SC), human brain-derived neurotrophic factor (h-BDNF, Cell Signaling Technology, 3897S), or human neurotrophin-3 (h-NT-3, Cell Signaling Technology, 5237SC) were added at a concentration of 5ug/mL before imaging.

2-3: Crosslinking

HEK293T cells were transfected with 2ug of Trk-eYFP DNA. A membrane impermeable crosslinker, BS^3 (bis(sulfosuccinimidyl) suberate; ThermoFisher Scientific, 21580), was used in the crosslinking experiments. Twenty four hours after transfection with Trk-A-YFP DNA, cells were incubated with 2 mM BS^3 for 1 hour at room temperature. The reaction was quenched with 20 mM Tris-HCl for 15 min. The cells were rinsed with ice-cold 1X PBS before lysing. In some

cases, cells were incubated with the neurotrophin hß-NGF (5ug/mL) for 10–15 min before adding the crosslinker. The lysates were subjected to SDS-PAGE, and the proteins were transferred to a nitrocellulose membrane. Trk-A-eYFP was probed using anti-GFP antibody (Cell Signaling Technologies, 2555S) as the primary antibody, followed by anti-rabbit HRP conjugated antibody (Promega, W4011). The membrane was incubated with Amersham ECL Plus ™ (GE HealthCare Life Sciences, RPN2106) for 2 min and exposed to detect the chemiluminescent signal in a Chemidoc imaging system (Bio-Rad).

2-4: Swollen Cells as Model System

Following published protocols [3][4][5], experiments were performed in HEK293T cells under reversible osmotic stress as shown in figure 2-3. The reversible osmotic swelling was necessary because the cell membrane of live cells is highly "wrinkled," while the reversible osmotic stress eliminates these ruffles [6]. Thus, the effective 3D protein concentration, determined using purified fluorescent protein standards of known concentration, can be converted into 2D receptor concentrations in the plasma membrane as previously described [3]. Before imaging, the serum-free media was replaced with hypotonic swelling media (1:9 serum-free media: diH_2O, 25mM HEPES) to induce reversible osmotic stress. Typically, imaging sessions started 10 min after the addition of the swelling buffer, and lasted about 2 hours. In some cases, neurotrophins were added to the swelling media prior to imaging.

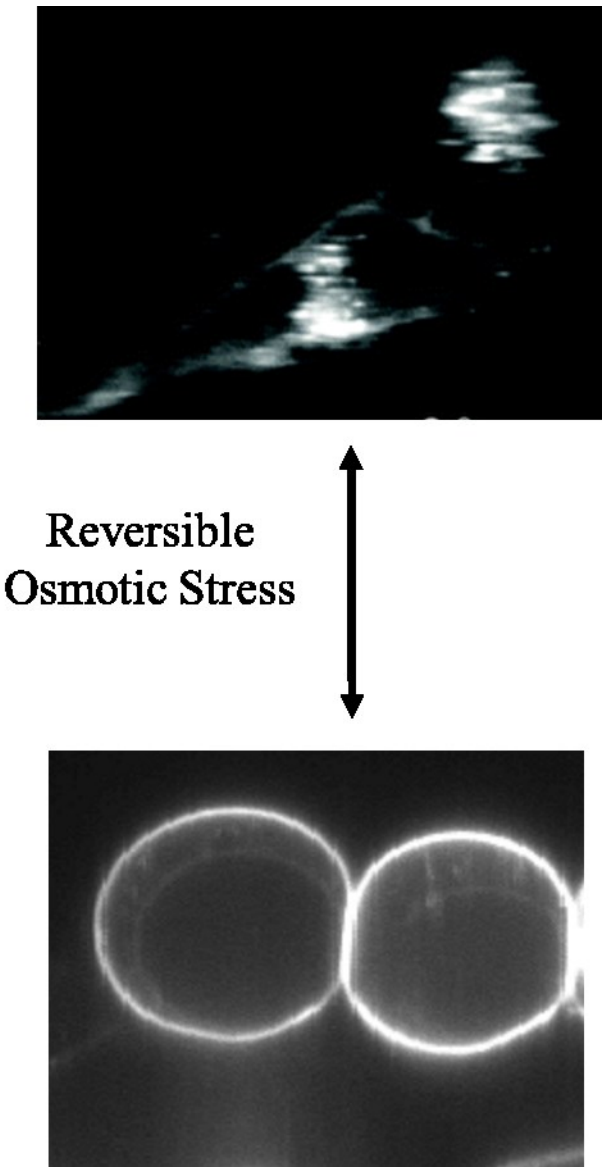

Figure 2- 3: HEK293T cells under reversible osmotic stress. Top: Non-swollen cell imaged in the two photon microscope. Bottom: Swollen cells imaged in the two photon microscope.

2-5: Image Acquisition by Two Photon Microscopy

A two photon microscope was used to acquire images of the swollen HEK293T cells. This system is equipped with a Mai Tai laser (Spectra-Physics, Santa Clara), used to generate femtosecond mode locked pulses and excite the fluorophores, and the OptiMis detection unit (Aurora Spectral Technology) which yields full fluorescence spectra for every pixel in the image. This microscope offers pixel level spectral resolution and line-scanning excitation capabilities [7]. Two images were acquired for each cell: one upon excitation at 800 nm to primarily excite the mTurq (donor), and a second one at 960 nm to primarily excite the eYFP (acceptor)[7]. The FSI-FRET method was used to measure the FRET efficiency, the donor (Trk-mTurq) concentration, and the acceptor (Trk-eYFP) concentration in small membrane areas of a cell as shown in Figure 2-4. More than 500 cells were analyzed in each case. To convert pixel level intensities of the images into concentrations, calibration solutions of purified fluorescent proteins were used as previously described [3]. Soluble eYFP and mTurquoise were produced following a previously published protocol [8].

A

Single transfected cell with mTurq construct

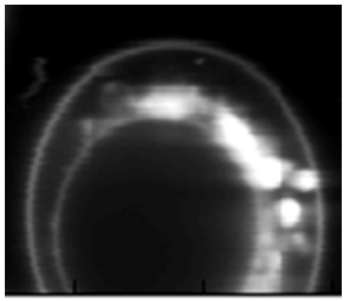

mTurq Spectra

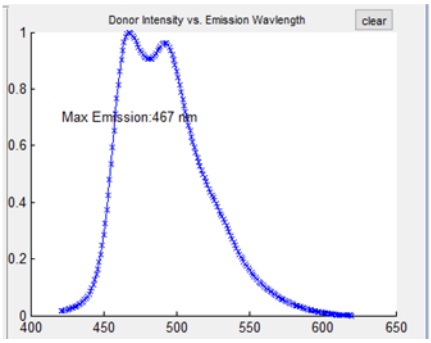

B

Single transfected cell with eYFP construct

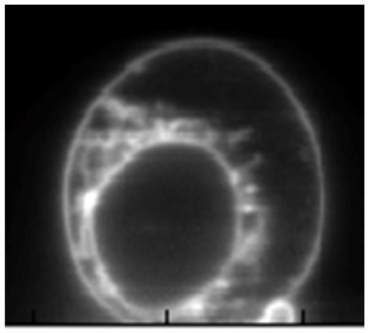

YFP Spectra

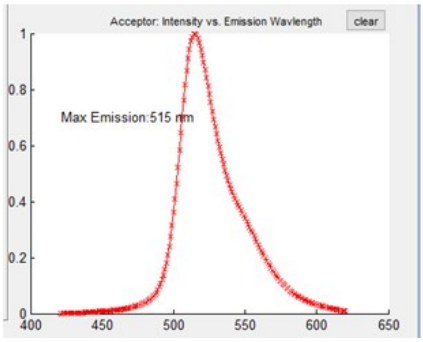

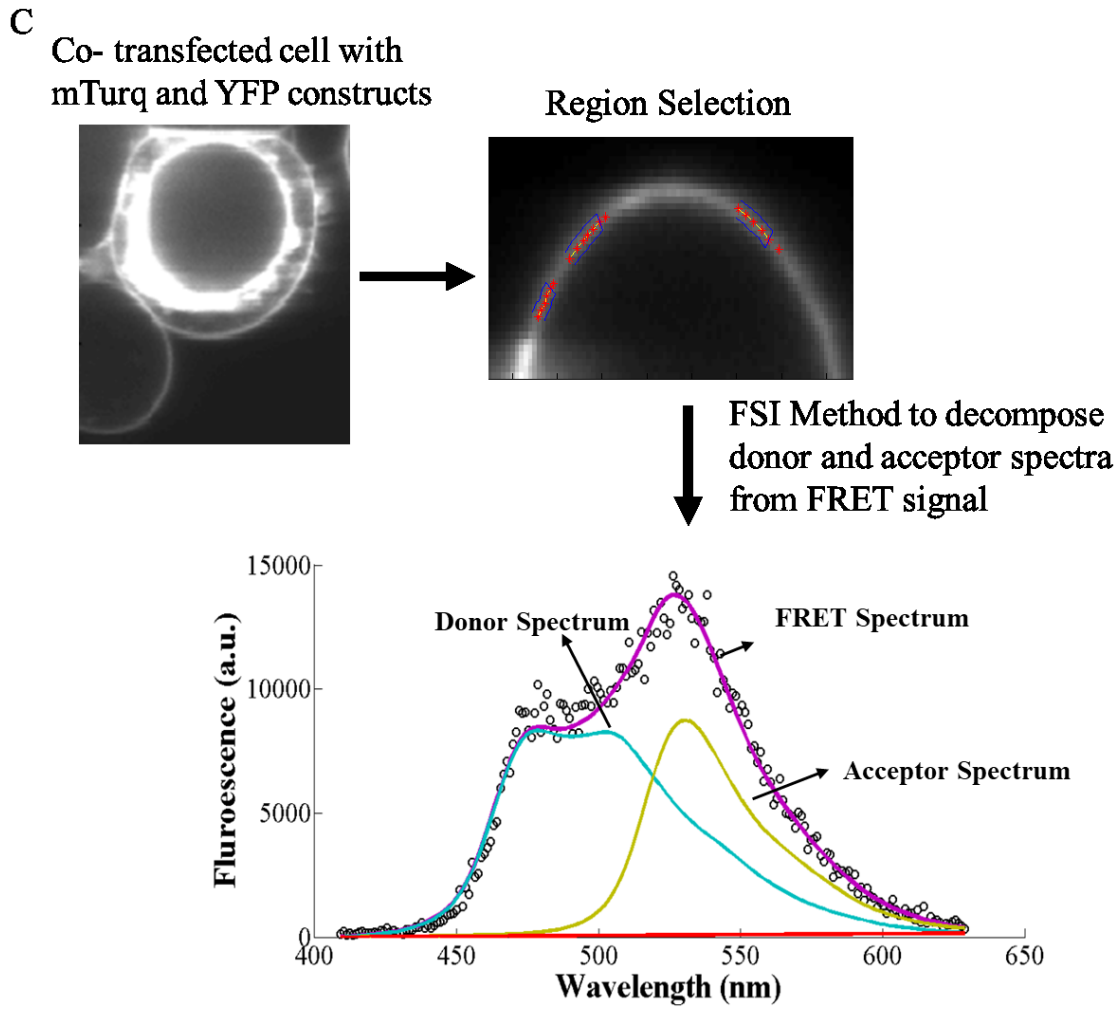

Figure 2- 4: The fully quantified spectral Imaging (FSI) method was used to unmix pixel-level FRET spectra. A: Cells expressing Trk-mTurq are used to obtain the mTurq spectra. B: Cell expressing Trk-eYFP are used to obtain the eYFP spectra. C: In cells expressing both Trk-mTurq and Trk-eYFP, regions were selected and the FSI method was used to decompose the FRET spectra into donor and acceptor contributions. This allows us to determine the FRET efficiencies, the donor concentrations, and the acceptor concentrations in each selected region of the cell.

2-6: Image Analysis

Analysis of the acquired images is done using the Fully Quantified Spectral Imaging (FSI) method [3]. We use images of calibration solutions containing pure soluble donors and acceptors at known micromolar concentrations to calculate donor and acceptor concentrations in the membrane. We fit the raw FRET data while varying two parameters: the intrinsic FRET ($\tilde{E}$), which is a structural parameter, and the equilibrium association constant (K) to generate dimerization curves.

The measured FRET efficiency has contributions due to both (i) specific dimerization of the Trk receptors, E_D and (ii) stochastic or "proximity FRET" that arises due to the random proximity of donors and acceptors in the two dimensional membrane, E_{prox} [9][10]. FRET measurements are corrected for the random, non-specific close proximity of the donors and acceptors using computer simulated FRET [11]. Thus, the measured (apparent) FRET efficiency E_{app} in the experiment is described by the following equation:

$$E_{app} = \frac{E_{prox} + E_D - 2E_{prox}E_D}{1 - E_D E_{prox}} \qquad (1)$$

2-7: Monomer-Dimer Model

We consider a monomer-dimer model to describe the equilibrium between monomers and dimers as follows:

$$m + m \overset{K}{\leftrightarrow} D \qquad (2)$$

Here (m) denotes monomers and (D) denotes dimers.

The equilibrium association constant (K) can be written as follows for the above reaction:

$$K = \frac{[D]}{[m]^2} \qquad (3)$$

The concentration of monomers $[m]$ can be written in terms of the equilibrium constant and the total concentration. First we solve for the fraction of monomers (f_m):

$$f_m = \frac{1}{1+2K[m]} \qquad (4)$$

We know that the total concentration $[T]$ can be written as:

$$[T] = [m] + 2[D] \qquad (5)$$

Substituting for $[D]$, we write $[T]$ as shown below:

$$[T] = m + 2[m]^2K \qquad (6)$$

We can use the quadratic equation to solve for the concentration of monomers $[m]$:

$$[m] = \frac{\sqrt{1 + 8K[T]} - 1}{4K} \qquad (7)$$

$$f_m = \frac{1}{1+2K[m]} = \frac{2}{\sqrt{1+8K[T]}+1} \qquad (8)$$

Next, we use the fact that the fraction of dimers plus the fraction of monomers is equal to 1, and calculate the fraction of dimers f_d as:

$$f_d = 1 - f_m = \frac{\sqrt{1+8K[T]}-1}{\sqrt{1+8K[T]}+1} \qquad (9)$$

The apparent FRET (E_{app}) due to dimer formation can be calculated as:

$$E_{app} = f_d x_A \tilde{E} \qquad (10)$$

Note that when the dimeric fraction is 100% (f_D=1), equation (2) reduces to

$$E_D = x_A \tilde{E} \qquad (11)$$

The equations above give us the relations needed to calculate the interaction parameters. The fraction of acceptors (x_A) is calculated by dividing the number of acceptors (A) by the total number of receptors (T) as:

$$x_A = \frac{A}{T} \qquad (12)$$

We use intrinsic FRET ($\tilde{E}$), which comes from fitting the model to the data, to calculate the distance between two fluorophores in the dimers as described below:

$$\tilde{E} = \frac{1}{1+\left(\frac{d}{R_0}\right)^6} \qquad (13)$$

The Förster radius (R_0) is unique to each donor/acceptor pair. The above equation uses $\tilde{E}$ and R_0 to yield the distance (d) between two fluorophores. In all cases, R_0 of 54.5Å is used to calculate the distance between two fluorophores attached to the Trk receptor in the plasma membrane.

Data fitting and analysis was performed by utilized a computationally-derived library of proximity FRET efficiencies that were simulated over a finite grid of equilibrium constant, K, and $\tilde{E}$ values, for acceptor concentrations ranging from zero to 8×10^3 acceptors/μm^2, and for three different exclusion radia: 1 nm, 1.4 nm, and 2 nm [10]. In the first step of the fitting procedure, this proximity FRET library was used to perform a gridded search for the best-fit K and $\tilde{E}$ from the library, by calculating the total FRET efficiencies and comparing them to the experimentally measured ones. Since small changes to these parameters have little effect on the magnitude of the proximity FRET contribution, in the second step we fixed the proximity contribution and we calculated the FRET efficiencies that are due to specific dimerization, E_D, using equation. We then fit a monomer-dimer model to the corrected FRET data while varying K_{diss} and $\tilde{E}$, using a MATLAB non-linear least squares algorithm to find the best-fit values of K_{diss} and $\tilde{E}$ and their 66% confidence intervals.

The stability of the dimer is related to the dissociation constant according to

$$\Delta G = RT \ln\left(K_{diss}/10^6\right) \qquad (14)$$

with K_{diss} reported in units of receptors per μm^2, and the standard state for ΔG calculation defined as $K^0_{diss} = 1$ rec/nm^2 [12]

2-8: Analysis of Variance (ANOVA)-Test

We performed one-way analysis of variance (ANOVA) to compare dimerization parameters for Trks in the absence and presence of ligands. The null hypothesis was tested that the dimerization parameter values are the same for the Trk receptors. A multiple comparisons test was performed to identify statistically significant differences among dimerization parameters. We utilized the Prism software to perform the ANOVA-testing.

2-9: References

[1] H. Yano, F. Cong, R. B. Birge, S. P. Goff, and M. V Chao, "Association of the Abl tyrosine kinase with the Trk nerve growth factor receptor.," *J. Neurosci. Res.*, vol. 59, no. 3, pp. 356–64, Feb. 2000.

[2] D. R. Singh, F. Ahmed, S. Sarabipour, and K. Hristova, "Intracellular Domain Contacts Contribute to Ecadherin Constitutive Dimerization in the Plasma Membrane.," *J. Mol. Biol.*, vol. 429, no. 14, pp. 2231–2245, 2017.

[3] C. King, M. Stoneman, V. Raicu, and K. Hristova, "Fully quantified spectral imaging reveals in vivo membrane protein interactions.," *Integr. Biol. (Camb).*, vol. 8, no. 2, pp. 216–29, Feb. 2016.

[4] D. R. Singh *et al.*, "Unliganded EphA3 dimerization promoted by the SAM domain.," *Biochem. J.*, vol. 471, no. 1, pp. 101–9, Oct. 2015.

[5] D. R. Singh, E. B. Pasquale, and K. Hristova, "A small peptide promotes EphA2 kinase-dependent signaling by stabilizing EphA2 dimers.," *Biochim. Biophys. Acta*, vol. 1860, no. 9, pp. 1922–8, 2016.

[6] B. Sinha *et al.*, "Cells respond to mechanical stress by rapid disassembly of caveolae.," *Cell*, vol. 144, no. 3, pp. 402–13, Feb. 2011.

[7] G. Biener *et al.*, "Development and experimental testing of an optical micro-spectroscopic technique incorporating true line-scan excitation.," *Int. J. Mol. Sci.*, vol. 15, no. 1, pp. 261–76, Dec. 2013.

[8] S. Sarabipour, C. King, and K. Hristova, "Uninduced high-yield bacterial expression of fluorescent proteins.," *Anal. Biochem.*, vol. 449, pp. 155–7, Mar. 2014.

[9] P. K. Wolber and B. S. Hudson, “An analytic solution to the Förster energy transfer problem in two dimensions.,” *Biophys. J.*, vol. 28, no. 2, pp. 197–210, Nov. 1979.

[10] C. King, S. Sarabipour, P. Byrne, D. J. Leahy, and K. Hristova, “The FRET signatures of noninteracting proteins in membranes: simulations and experiments.,” *Biophys. J.*, vol. 106, no. 6, pp. 1309–17, Mar. 2014.

[11] C. King, V. Raicu, and K. Hristova, “Understanding the FRET Signatures of Interacting Membrane Proteins.,” *J. Biol. Chem.*, vol. 292, no. 13, pp. 5291–5310, Mar. 2017.

[12] L. Chen, L. Novicky, M. Merzlyakov, T. Hristov, and K. Hristova, “Measuring the energetics of membrane protein dimerization in mammalian membranes.,” *J. Am. Chem. Soc.*, vol. 132, no. 10, pp. 3628–35, Mar. 2010.

Chapter 3: Dimerization of the Trk receptors in the plasma membrane: effects of their cognate ligands

This article was published in the Biochemical Journal. The text here is revised to match the thesis submission requirement.

Ahmed, Fozia, and Kalina Hristova. "Dimerization of the Trk receptors in the plasma membrane: effects of their cognate ligands." *Biochemical Journal* 475.22 (2018): 3669-3685.

3-1: Introduction

RTKs, the second largest family of membrane receptors, are known to control cell growth, differentiation, and motility via lateral dimerization in the membrane. Their dysregulation has been linked to many human diseases and disorders, including a variety of cancers [1][2][3][4]. There are 58 different RTKs in humans, grouped in 20 different families, which all share the same basic architecture: an N-terminal extracellular (EC) region, a single-pass transmembrane (TM) domain, and an intracellular (IC) region containing a tyrosine kinase domain [5]. The RTK ligands are polypeptides often referred to as "growth factors." The ligands bind to the RTK EC regions and activate the kinases, via a process that involves their cross-phosphorylation on specific tyrosine residues. The activated kinases then phosphorylate additional tyrosines that serve as docking sites for adaptor proteins. The adaptors, in turn, bind cytoplasmic substrates and trigger downstream signaling pathways [1][6][7][8][9][10], such as the MAPK, PI3K, PKC, and STAT cascades which impact growth, development, and disease progression.

Work during the last decade has provided evidence that RTK dimerization is required, but is not sufficient, for RTK activation. Instead, there also exist structural requirements for cross-phosphorylation to occur [2][11][12][13]. In particular, it has been proposed that a specific

orientation of the kinase domains in the dimer is required, and this optimal orientation is achieved only upon ligand binding, as a result of structural rearrangements that propagate along the length of the RTK[14][15][16].This view is supported by experiments which show that the TM domain dimer conformation changes upon ligand binding, correlating with an increase in receptor phosphorylation [17][18] Furthermore, the rotation of the TM dimer interface has been shown to lead to periodic oscillations in kinase activity, suggesting that the TM dimer structure is sensed by the kinases [19].

An alternate view exists, however, that ligand-induced structural changes cannot be propagated along the length of the RTK because the linkers between the different domains are unstructured [20]. In support of this view, there are data suggesting that the EC and IC domains can change conformations independently of each other [21][22]. There is also structural evidence for a loose connection between the EC and TM domains [22][23]. Within this conceptual framework, the main role of the ligand is to increase the stability of the RTK dimer [24]. Thus, there is no consensus on the mechanism of RTK activation by their ligands, even after decades of RTK research.

Here, we investigate the interactions that regulate the behavior of the three RTKs from the Tropomyosin Receptor Kinase (Trk) family in the plasma membranes of mammalian cells. The Trk receptors are expressed in neuronal tissues, and they guide the development of the central and peripheral nervous systems [25][26][27]. They also play a profound role in disease, such as cancer and neurodegeneration [28][29][30]. The Trk receptors share a high degree of structural homology, and their extracellular domains are all composed of three leucine-rich motifs flanked by two cysteine-rich clusters at the N-terminus, followed by two Ig-like domains linked to the TM segment. The ligands of the Trk receptors are called neurotrophins. They bind to the second Ig-

like domain closest to the membrane, and trigger downstream ERK, PI3K and PLC-γ signaling pathways that control differentiation, proliferation, and survival of neurons [31][32][33][34].

The biology of the Trk receptors has been studied extensively, because of their important physiological roles [25][26][35]. However, the biophysical principles behind Trk receptor dimerization and activation in response to their ligands have not been elucidated. We characterize the homodimerization of the three Trk receptors in the plasma membrane, as well as their response to their cognate ligands (hß-NGF in the case of Trk-A, h-BDNF in the case of Trk-B, and h-NT-3 in the case of Trk-C). We do this with the help of a FRET-based methodology that can give quantitative information about RTK dimerization, and can report on structural changes that occur in the RTK dimer upon ligand binding [36][37][38][39].

3-2: Results

Full length Trk-A forms dimers in the plasma membrane, in the absence of ligand

To study Trk receptor dimerization using FRET, we attached either mTurquoise or eYFP (a FRET pair) to the C-terminus of full length Trk-A (Figure 2-2). Then, we co-transfected HEK 293T cells with 2 ug of DNA encoding for Trk-A-mTurquoise and Trk-A-eYFP, while varying the ratios of the two plasmids. After the receptors were trafficked to the plasma membrane, the cells were starved for 12 hours to remove all ligands, and imaged in a two photon microscope equipped with the OptiMiS spectral detection system [39][40]. Images were acquired and processed using the fully quantified spectral imaging (FSI) methodology, which involves the acquisition of two complete spectra: a FRET spectrum collected upon donor excitation, and an acceptor spectrum collected upon acceptor excitation [39]. As discussed in details in previous work [39], the FSI methodology yields FRET efficiencies and receptor concentrations in the plasma membrane with high precision, and can thus yield dimerization curves.

It is a challenge to measure the two-dimensional (2D) concentration of membrane proteins in the plasma membrane, because cells possess two to three times the membrane surface needed to sustain their shape and thus the plasma membrane is highly "wrinkled" or "ruffled" [41][42]. While the effective 3D receptor concentrations can be determined by comparing the fluorescence intensities with standard solutions of fluorescent proteins of known concentrations [37][38], the complex membrane topology prevents their conversion into 2D receptor concentrations within the plasma membrane [43]. However, cell membranes can be "un-wrinkled" in a reversible manner when the cells are subjected to controlled osmotic stress which leads to the disassembly of the caveolae [44]. The application of the reversible stress does not alter the FRET efficiencies [45], indicating that membrane protein interactions are not altered in a measurable way. The reversible stress does not cause irreversible cell damage, either [46],[47]. In the cells under reversible osmotic stress, we analyzed membrane regions of homogenous fluorescence, about 3 μm in length, using the FSI software [39]. We calculated three parameters for each of the regions: the donor concentrations, the acceptor concentrations, and the FRET efficiencies [39].

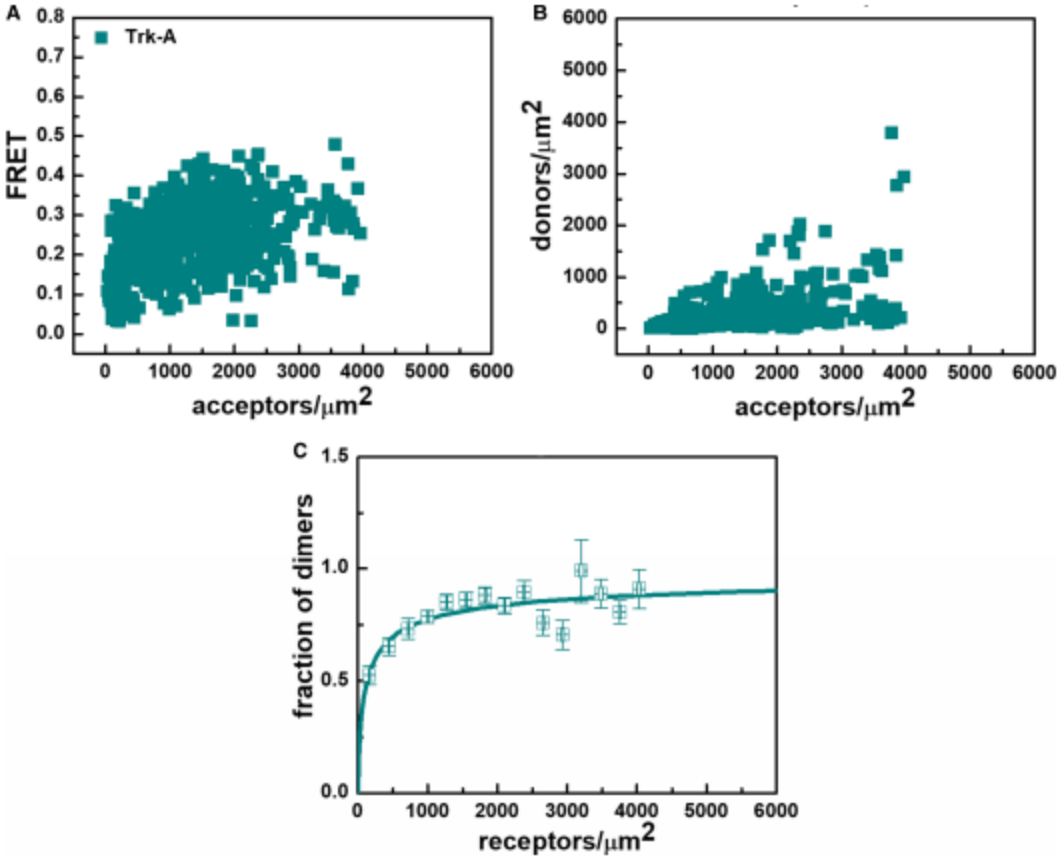

Figure 3- 1: FRET data for full-length Trk-A in the absence of ligand. (A) FRET efficiencies as a function of acceptor (Trk-A-eYFP) concentration. Every data point has different donor (Trk-A-mTurquoise) concentration. (B) Donor (Trk-A-mTurquoise) concentration, plotted as a function of acceptor (Trk-A-eYFP) concentration. (C) Fraction of Trk-A dimers as a function of total Trk-A concentration. The experimentally determined dimeric fractions are binned and are shown with the symbols, along with the standard errors. The solid line indicates the best-fit dimerization curve, plotted for the best-fit K_{diss} shown in Table 3-1.

The Trk-A FRET data, for the case of the 1:3 donor-to-acceptor transfection ratio, is shown in figure 3-1. Figure 3-1-A shows the FRET efficiencies as a function of acceptor concentration. Figure 3-1-B shows the donor versus the acceptor concentration in each region. Since each data point is derived from one cell, Figure 3-1-B demonstrates that the analyzed cell pool exhibits a substantial variation in the donor-to-acceptor ratio and the total receptor concentration (donor + acceptor expression) despite the fact that transfection is always performed under identical conditions. This heterogeneity is embraced and exploited in the FSI-FRET method, as it enables robust fits of thermodynamic models to the FRET data [38][45][48][49][50].

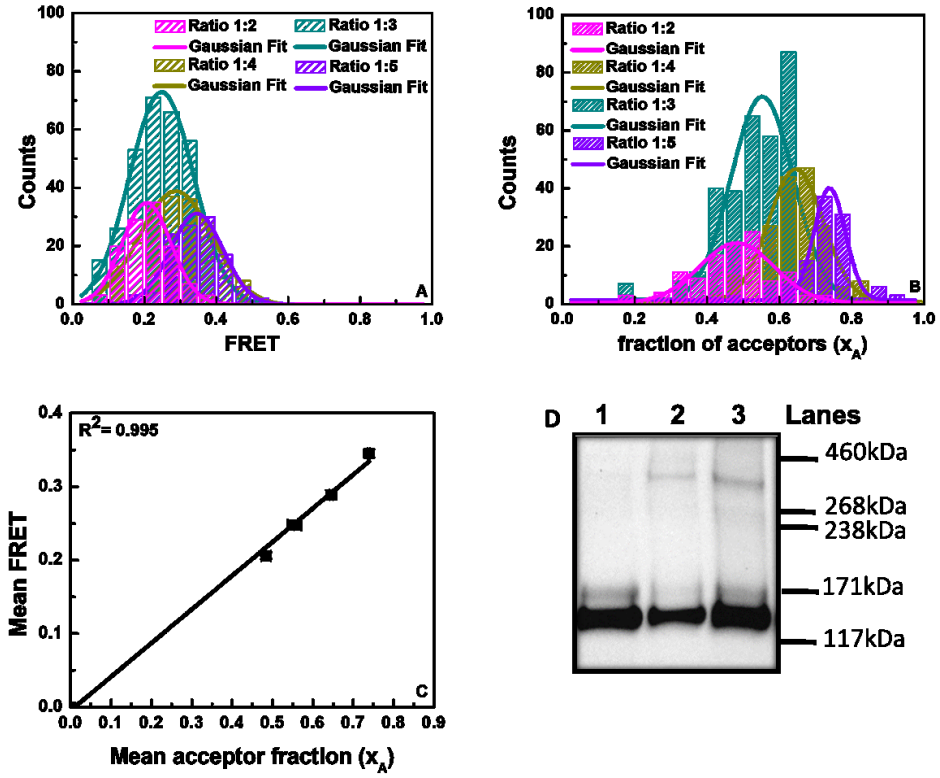

Figure 3- 2: FRET and cross-linking data demonstrating full-length Trk-A dimer-formation. (A) Histograms of measured FRET efficiencies at four different donor to acceptor ratios (1:2, 1:3, 1:4, and 1:5). (B) Histograms of acceptor fractions (x_A) for the four donor to acceptor ratios. (C) Average FRET efficiencies as a function of average acceptor fractions (x_A). The standard errors, which are smaller than the symbols, are also shown. The linear dependence is indicative of dimer formation. (D) Trk-A Western blot in the absence and presence of a chemical cross-linker. Lane 1: Trk-A; Lane 2: Trk-A + cross-linker; Lane 3: Trk-A + hß-NGF + cross-linker. The molecular weight of monomeric, mature, fully glycosylated TrkA is ~ 140 kDa, and thus the molecular weight of fully mature Trk-A-YFP is ~170 kDa. The intense lower molecular weight band corresponds to immature, partially glycosylated TrkA found in the ER and Golgi. The fully mature Trk-A-YFP dimer molecular weight is ~340 kDa.

Most RTKs are known to form dimers, and we investigated if this is the case for Trk-A by examining the dependence of the FRET efficiency on the acceptor fraction. In this type of analysis, the dependence of the FRET efficiency on the acceptor fraction is known to be linear for a dimer and nonlinear for higher order oligomers [47], [51], [52], [53]. To investigate this dependence, we analyzed the FRET efficiencies measured for four different Trk-A-mTurquoise to Trk-A-eYFP DNA transfection ratios: 1:2, 1:3, 1:4, and 1:5 (shown in Figure 3). Histograms of FRET efficiencies and fractions of acceptor-labeled receptors are shown in Figure 3-2-A and 3-2-B for the four different transfection ratios. These histograms were fitted to Gaussian functions to obtain the averages and the standard errors. The average FRET efficiencies obtained from the histograms are plotted versus the average acceptor ratios in Figure 3-2-C for the four DNA transfection ratios (symbols; standard errors are also shown but they are smaller than the symbols). The data in Figure 3-2 are well described by a linear function (R^2=0.995), suggesting that Trk-A forms dimers in the absence of ligand.

To confirm dimer formation, we performed cross-linking experiments with Trk-A-eYFP in the presence and absence of its ligand hß-NGF. In these experiments, cells expressing Trk-A-eYFP were incubated with a cross-linker, lysed, and subjected to Western blotting. Since in the cross-linking experiments we do not monitor the 2D concentrations of the receptors in the membrane, no application of reversible osmotic stress was required. Trk-A bands were visualized using anti-GFP antibodies. Results, shown in Figure 3-2-D, reveal two monomeric bands: one at molecular weight ~170 kDa, corresponding to mature, fully glycosylated Trk-A-YFP, and one at ~140 kDa, corresponding to immature, partially glycosylated Trk-A-YFP found in the ER and the Golgi [54], [55]. The dimer band for the fully glycosylated Trk-A-YFP is expected to be at ~340 kDa, and indeed we see such a band in the presence of the cross-linker. These results support the

idea that Trk-A forms a dimer, in the absence and presence of ligand, and are consistent with the literature [56]. Note that the immature band is not cross-linked because it is not localized to the plasma membrane (as the cross-linker is membrane-impermeable), and thus does not contribute to the measured FRET in figures 3-1 and 3-2.

Next, we sought to interpret the FRET data in figure 3-2 within the framework of a thermodynamic model of dimerization as described previously [43]. Dimer formation can be characterized by two parameters: the two-dimensional dissociation constant, $K_{diss,}$ and the structural parameter $\tilde{E}$ (or "Intrinsic FRET"). The dissociation constant, K_{diss}, is a measure of the dimerization propensity of Trk-A in the plasma membrane. The Intrinsic FRET is the FRET efficiency in a Trk-A dimer with one donor and one acceptor. It depends on the positioning of the fluorescent proteins within the Trk-A dimer, but not on the dimerization propensity [17], [37]. To interpret the FRET data, we further took into account that the measured FRET in the membrane has two contributions: one due to Trk-A dimerization and one due to the confinement of the mobile fluorophores in the two-dimensional membrane [57],[43]. The latter FRET occurs because of the random close approach (within 100 Å) of the donors and acceptors in the plasma membrane. This "proximity FRET" contribution is well understood, and can be corrected for as discussed in detail elsewhere [57], [43], [58]. The best-fit K_{diss} and the best-fit Intrinsic FRET are determined from the FRET data while accounting for proximity FRET, following a verified two-step fitting protocol that is briefly described in Materials and Methods (see also [58]). The dimeric fraction of Trk-A as a function of the total Trk-A concentration is shown in Figure 2C. We see that Trk-A exhibits a significant dimer population in the absence of ligand. The solid line in Figure 2C shows the dimerization curve calculated for the best-fit value of K_{diss}. The solid symbols show the

experimentally derived dimeric fractions, which have been binned into 30 bins over the expression range of Trk-A, and then averaged within the bins.

The optimal values of K_{diss} and Intrinsic FRET, as well as their 66% confidence intervals, are given in Table 3-1. The two dimensional dissociation constant for the Trk-A receptor, K_{diss}, is 132 ± 0.37 receptors/μm^2, and the corresponding dimerization free energy is -5.30 ± 0.17 kcal/mole. The Trk-A Intrinsic FRET value in the absence of ligand is 0.33 ± 0.01.

Constructs	K_{diss} (rec.µm^{-2})	ΔG (kcal/mol)	Intrinsic FRET (Ẽ)	d(Å)
Trk-A	132 ± 37	-5.30 ± 0.17	0.33 ± 0.01	61 ± 1
Trk-A+ hß-NGF	100% dimer	n.d.	0.28 ± 0.02	64 ± 1
Trk-B	12 ± 2	-6.72 ± 0.10	0.35 ± 0.04	60 ± 2
Trk-B+ h-BDNF	100% dimer	n.d.	0.30 ± 0.02	63 ± 1
Trk-C	227 ± 25	-4.98 ± 0.07	0.88 ± 0.02	39 ± 1
Trk-C+ h-NT-3	100% dimer	n.d.	0.64 ± 0.03****	50 ± 1

Table 3- 1: Dimerization parameters for the three full-length Trk receptors, in the absence of ligand and in the presence of 380 nM ligand. Kdiss is the two-dimensional dissociation constant, a thermodynamic parameter, which is related to the stability of the Trk dimers, ΔG, according to equation 14. Ẽ is the Intrinsic FRET, which depends on the positioning of the fluorescent proteins within the Trk dimers. The average distance between the fluorescent proteins, d, is calculated from Ẽ using equation 13, under the assumption for free rotation of the fluorescent proteins (n.d. not determined; ****p-Value <0.0001).

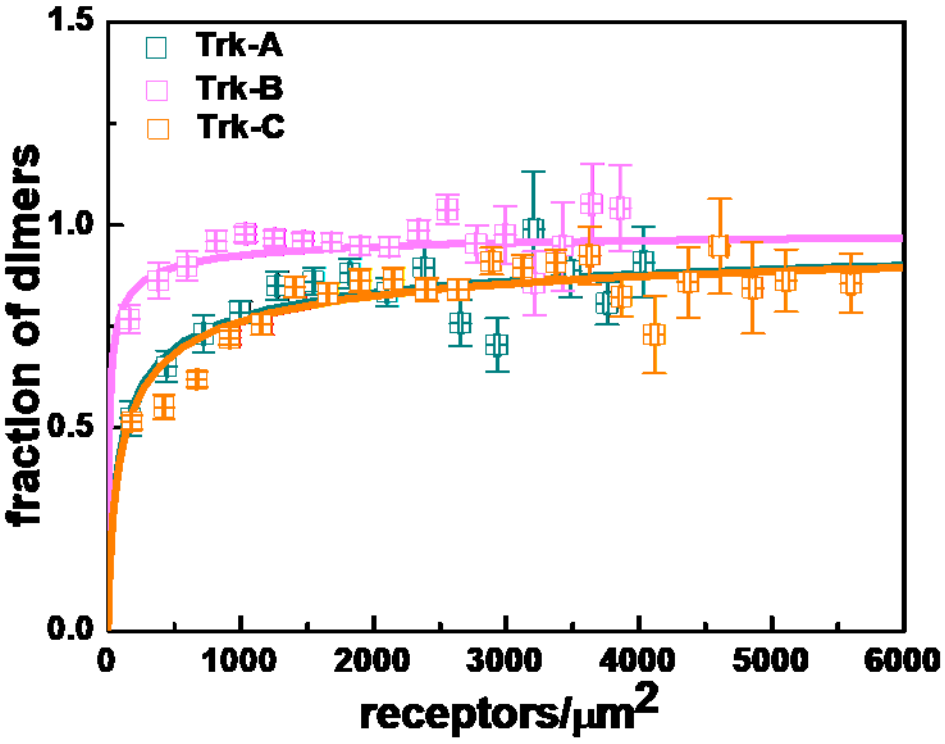

Figure 3- 3: Dimerization curves for the three full-length Trk receptors in the absence of ligands. The best-fit dimerization parameters are shown in Table 3-1.

Full length Trk-B and Trk-C receptors form dimers in the plasma membrane, in the absence of ligand

We performed similar experiments with full-length Trk-B and Trk-C, labeled with either mTurquoise or eYFP at their C-termini via flexible $(GGS)_5$ linkers. The dimerization curves, obtained as described above, are shown in figure 3-3, and are compared to the Trk-A results. The two parameter fit to the Trk-C data reveals a dimerization constant that is similar to Trk-A, but the value of the Intrinsic FRET is higher (Table 3-1). Trk-B, on the other hand, exhibits much higher dimerization propensity, with $K_{diss} = 12 \pm 2$ rec/μm^2. Overall, the data in figure 3-3 show that all three Trk receptors, and particularly Trk-B, homo-dimerize strongly in the plasma membrane, even in the absence of ligand.

Thermodynamic contributions of Trk domains to unliganded dimerization

In order to gain insight into the contributions of the different domains to the stability of the unliganded Trk-A dimer, two truncated versions of the Trk-A receptor were created. First, the IC domain was removed to generate a Trk-A ECTM construct containing the EC and TM domains, with the fluorescent proteins attached to the TM domains via a 15 amino acid $(GGS)_5$ flexible linkers [59], [60] (see Figure 2-2). In the second truncated version of the Trk-A receptor, both the IC and EC domains were removed to generate the TM Trk-A construct, with the fluorescent proteins attached to the TM domain C-terminus by the same 15 amino acids $(GGS)_5$ flexible linker (Figure 2-2). The FSI method was used to characterize the dimerization of the two truncated Trk-A constructs.

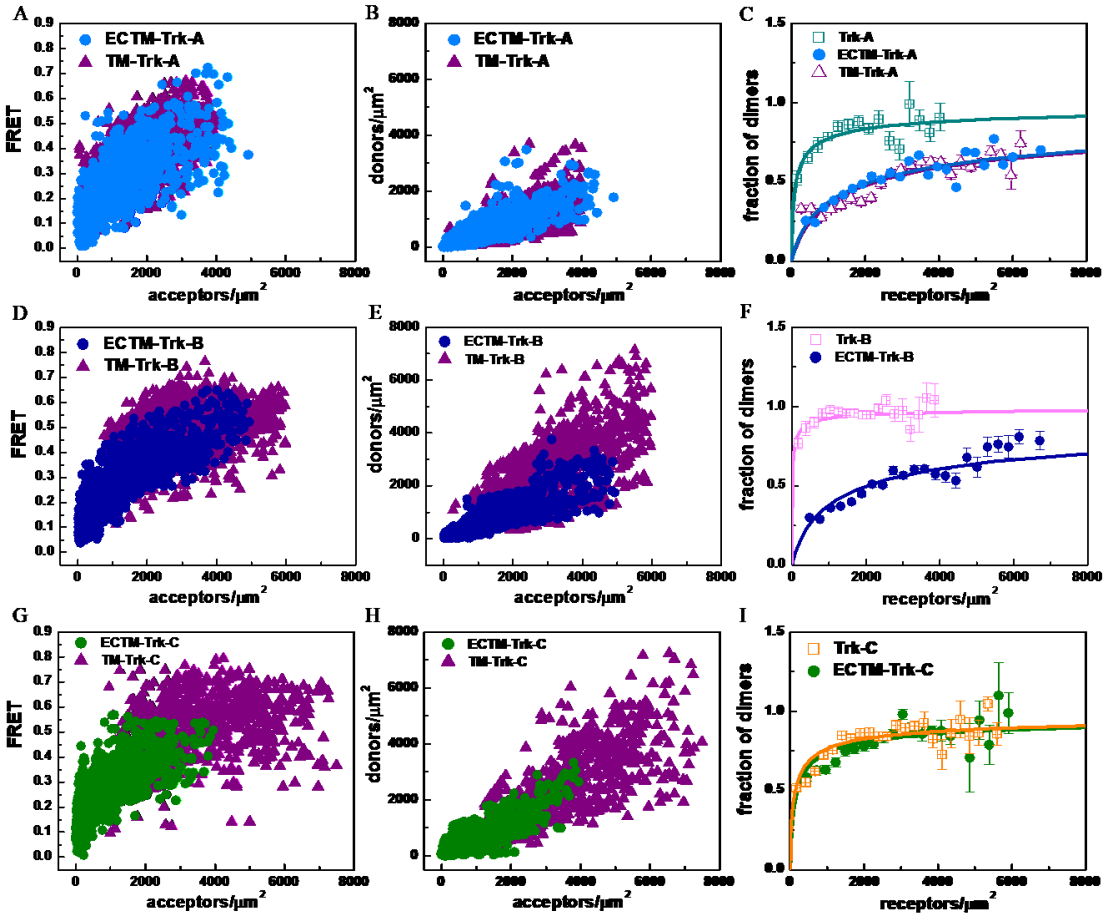

Figure 3- 4: FRET data for the ECTM Trk receptors, which lack IC domains, and for the TM Trk receptors, which lack both EC and IC domains. Data are collected in the absence of ligand. (A, D, and G) Measured FRET efficiencies as a function of receptor concentrations. (B, E, and H) Donor concentrations versus acceptors concentrations. (C, F, and I) Dimeric fractions as a function of total receptor concentrations. The experimentally determined dimeric fractions are binned and are shown with the symbols, along with the standard errors. The solid lines are the dimerization curves, plotted for the optimized dimerization parameters reported in Table 3-2. The FRET data for the TM Trk-B and Trk-C constructs could not be fitted with a dimer model.

Constructs	K_{diss} (rec/μm^2)	ΔG (kcal/mol)	Intrinsic FRET (Ẽ)	d(Å)
TM-Trk-A	2271 ± 310	-3.61 ± 0.09	0.96 ± 0.03	32 ± 5
ECTM-Trk-A	2127 ± 278	-3.65 ± 0.08	0.76 ± 0.04	45 ± 2
ECTM-Trk-A + hß-NGF	25 ± 5	-6.28 ± 0.12	0.59 ± 0.01****	51 ± 1
ECTM-Trk-B	2018 ± 134	-3.68 ± 0.04	0.82 ± 0.02	42 ± 1
ECTM-Trk B + h-BDNF	23 ± 2	-6.33 ± 0.06	0.50 ± 0.01****	55 ± 1
ECTM-Trk-C	183 ± 29	-5.10 ± 0.09	0.57 ± 0.01 n.s	52 ± 1
ECTM-Trk-C + h-NT-3	15 ± 4	-6.59 ± 0.16	0.64 ± 0.01	50 ± 1

Table 3- 2: Dimerization parameters for the three truncated Trk receptors, in the absence of ligand and in the presence of 380 nM ligand (n.s. not statistically significant; ****p-Value <0.0001).

Figure 3-4-A shows FRET as a function of acceptor concentration for the ECTM and TM Trk-A constructs. Figure 3-4-B shows the donor versus the acceptor concentration for these constructs. Figure 3-4-C compares the dimerization curves for the ECTM and TM constructs with the dimerization curve for the full length Trk-A receptor. The calculated best-fit parameters for these constructs are reported in Table 3-2. According to these results, the removal of the IC domain decreases the dimer stability from -5.30 ± 0.17 to -3.65 ± 0.08 kcal/mole, indicating that contacts involving the IC domains stabilize the full-length Trk-A dimer. The removal of the EC domain, however, has no effect on dimer stability, as the ECTM and TM free energies of dimerization are the same, -3.65 ± 0.08 and -3.61 ± 0.09 kcal/mole, respectively. Thus, Trk-A dimerization in the absence of ligand occurs because of stabilizing contacts between the TM and IC domains, without a significant contribution from the EC domain.

We performed similar experiments with the truncated versions of Trk-B and Trk-C. Figures 3-4-D and 3-4-G show FRET as a function of acceptor concentration. Figures 3-4-E and 3-4-H show the donor versus the acceptor concentration for these constructs. Figures 3-4-F and 3-4-I compare the dimerization curves for the ECTM and full-length receptors. According to the best-fit parameters in Table 3-1 and Table 3-2, the removal of the IC domain in Trk-B decreases the dimer stability from -6.72 ± 0.10 to -3.68 ± 0.04 kcal/mole, while the IC domain in Trk-C has no significant effect on dimerization. Of note, attempts to fit the FRET data for the Trk-B and Trk-C TM constructs with a dimer model were unsuccessful, suggesting that these TM domains form oligomers in the plasma membrane.

Effect of ligands on Trk dimerization

Neurotrophins interact with the Trk receptors to initiate downstream signaling [25][31] [61]. Here we studied how Trk dimerization is affected by three ligands, hß-NGF, h-BDNF, and

h-NT-3, which are known as cognate ligands for Trk-A, Trk-B, and Trk-C, respectively. The ligand binding affinities have been characterized previously using different methods, and published values are in the pM to low nM range [26][62][63][64][65][66].

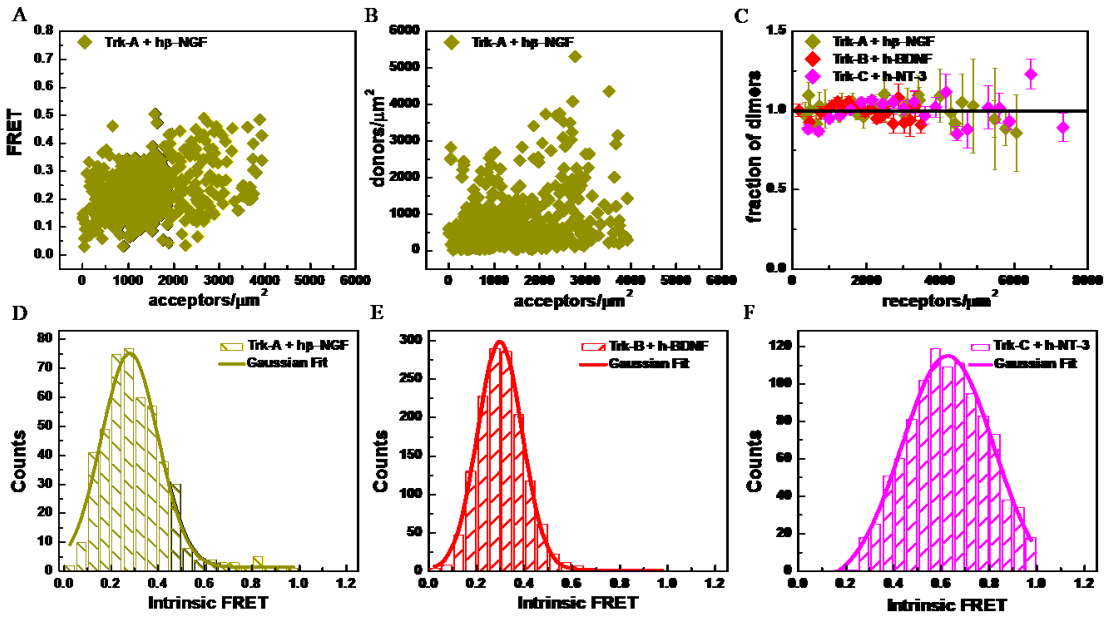

Figure 3- 5: FRET data for full-length Trk receptors in the presence of ligand at saturating concentration. (A) FRET as a function of acceptor concentration for Trk-A in the presence of hß-NGF. (B) Trk-A-mTurquoise (donor) concentration versus Trk-A-eYFP (acceptor) concentration in the presence of hß-NGF. (C) Fraction of dimers as a function of total receptor concentration for Trk-A, Trk-B and Trk-C in the presence of hß-NGF, h-BDNF and h-NT-3, respectively. (D) Histogram of Trk-A Intrinsic FRET values in the presence of hß-NGF. (E) Histogram of Trk-B Intrinsic FRET values in the presence of h-BDNF. (F) Histogram of Trk-C Intrinsic FRET values in the presence of h-NT-3. The dimerization parameters for the three receptors in the presence of ligands are reported in Table 3-1.

We sought to carry out FRET experiments under well-defined conditions, when all the Trk receptors are ligand-bound. We therefore performed the FRET experiments in the presence of 5 ug/ml (~ 380 nM) of each ligand, which greatly exceeds the reported dissociation constants. The FRET and concentration data for Trk-A in the presence of hß-NGF are shown in Figures 3-5-A and 3-5-B. The dimerization curves (dimeric fractions as a function of total Trk concentration) for the three Trk receptors are shown in Figure 3-5-C in the presence of their respective ligands. We see that the Trk receptors are 100% dimeric over the concentration range sampled in the experiments. Thus, the two-dimensional dissociations constants are very low and could not be measured. The results demonstrate that hß-NGF, h-BDNF, and h-NT-3 stabilize the Trk-A, Trk-B, and Trk-C dimers, respectively.

In the case of 100% dimers, the Intrinsic FRET is calculated for each cell using equation 11. Note that both the FRET efficiencies and the acceptor fractions, x_A, are directly measured with the FSI-FRET method, and thus no fitting was required for these calculations. The Intrinsic FRET values from individual cells are shown as histograms in Figures 3-5D, E and F, for Trk-A, Trk-B, and Trk-C, respectively, and are fit with Gaussian functions. The Gaussian fit parameters are shown in Table 3-1. Comparison of the Intrinsic FRET values in Table 3-1 with and without ligand reveals a large change in Intrinsic FRET for Trk-C upon the addition of h-NT-3, but no significant effects for Trk-A and Trk-B in response to hß-NGF and h-BDNF, respectively. As the fluorescent proteins are attached to the C-termini via flexible linkers, the differences in Intrinsic FRET for Trk-C must reflect changes in the relative positioning of the C-termini of Trk-C upon h-NT-3 binding.

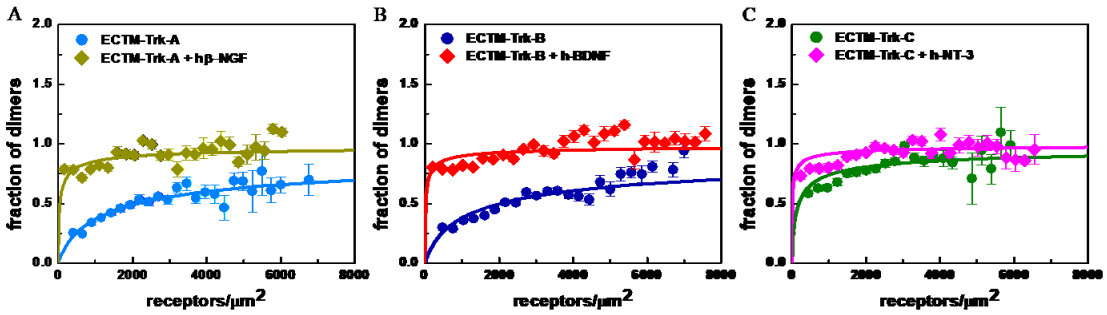

Figure 3- 6: Dimerization curves for ECTM Trk-A, Trk-B and Trk-C in the presence and absence of ligands. (A) ECTM Trk-A in the presence and absence of hß-NGF. (B) ECTM Trk-B in the presence and absence of h-BDNF. (C) ECTM Trk-C in the presence and absence of h-NT-3.

To gain additional insights into the effect of the three ligands on Trk dimerization, we performed FRET experiments with the truncated ECTM Trk constructs with deleted kinase domains, in the presence of ligands. The dimerization curves for the ECTM Trk receptors in the presence of saturating concentrations of their cognate ligands are shown in Figure 3-6 and are compared to the curves in the absence of ligand. The best fit dimerization parameters are shown in Table 3-2. Inspection of Figure 3-6 and Table 3- 2 shows that the cognate ligands stabilize the ECTM Trk dimers.

As the deletion of the IC domains decreases Trk dimerization, we are able to quantify the stabilities of the ligand-bound Trk dimers and to calculate the respective dissociation constants (see Table 3-2). This allows us to determine the effect of the bound ligands on the thermodynamic stabilities of the dimers, by subtracting the ECTM dimer stabilities with and without ligand. We see that hß-NGF, h-BDNF, and h-NT-3, at 380 nM, stabilize the Trk-A, Trk-B, and Trk-C dimers by -2.63 ± 0.14 kcal/mole, -2.65 ± 0.10 kcal/mole, and -1.49 ± 0.17 kcal/mole, respectively.

Table 3-2 shows the Intrinsic FRET values for the liganded truncated ECTM Trk dimers, determined from the fit of a monomer-dimer model to the measured FRET data. When we compare these values to the values in the absence of ligand, we see significant differences in the cases of Trk-A and Trk-B. As the fluorescent proteins are attached directly to the TM domains via flexible linkers, the changes in Intrinsic FRET likely reflect changes in the distance between the C-termini of the TM domains of Trk-A and Trk-B upon ligand binding [17][18][67].

3-3: Discussion

Experimental findings

Using a FRET-based quantitative technique, we showed that the Trk receptors form dimers not only in the presence of ligand, but also in the absence of ligand. Our results are consistent with the literature [56][68][69], and yield the first measurements of Trk dimer stabilities. The Trk dissociation constants in the unliganded case, which vary from 12 to 227 rec/μm^2, can be compared to the dissociation constants measured previously for the FGFRs— varying from 24 rec/μm^2 (for FGFR3) to 710 rec/μm^2 (for FGFR1) [17]—and for VEGFR2—35 rec/μm^2 [18]. Thus, the Trk receptor propensities for unliganded dimerization are similar to those of other characterized full length RTKs.

The estimates of Trk-A expression in the membrane of PC12 cells are ~20 Trk-A rec/μm^2 [69], [70]. Since the measured Trk-A dissociation constant is 132 ± 37 rec/μm^2, about 20% of the Trk-A molecules are expected to be dimeric in PC12 cells in the absence of ligand. Notably, Trk-A expression in PC12 cells is similar to the measured Trk-B dissociation constant, 12 ± 2 rec/μm^2. This suggests that unliganded Trk dimerization is important in physiological contexts.

To gain insight into factors that determine the stability of the unliganded Trk dimers, we measured the thermodynamic contributions of the different Trk domains to unliganded dimerization (Figure 3-4). The contributions of the IC domains of Trk-A and Trk-B to dimer stabilities are favorable, since the deletion of the IC domains significantly destabilized the Trk-A and Trk-B dimers. However, the contribution of Trk-C IC domain is practically zero, suggesting that either Trk-C IC domain does not engage in contacts that stabilize the full-length Trk-C dimer, or these stabilizing contacts are balanced by repulsive ones. This finding is reminiscent of the case

of the FGFRs, where the IC domains of FGFR2 and FGFR3 contribute to dimer stabilization, but the FGFR1 IC domain has no effect [17].

By measuring the dimerization of the TM Trk-A construct and comparing it to the ECTM Trk-A construct, we showed that the contribution of Trk-A EC domain to unliganded dimerization is negligible. This result is different from observations for other RTKs such as the FGFRs and VEGFR2, where removal of the EC domain increases dimer stability [17], [18], thus indicating that the EC domains of those other receptors inhibit dimerization in the absence of ligand. A crystal structure of the hß-NGF-bound isolated Trk-A EC domain shows that the ligand-bound dimer is stabilized exclusively through hß-NGF-TrkA contacts, but not through direct Trk-A—Trk-A contacts [71]. Accordingly, it appears that there are no direct interactions between Trk-A EC domains that contribute to dimer stability, both in the absence and presence of the hß-NGF ligand. The Trk-A dimers are instead stabilized through contacts between the TM domains and the IC domain.

Unlike in the Trk-A case, we were not able to determine the thermodynamic contribution of Trk-B and Trk-C EC domains to unliganded dimerization, because we could not fit the FRET data for TM Trk-B and TM Trk-C with a dimer model. Thus, these TM domains likely form oligomers that are larger than dimers. Despite the propensity of these TM domains to oligomerize, it can be expected that the bulky Trk-A EC and IC domains impose constraints that do not allow three or more TM helices to interact closely, thus preventing higher order oligomerization for the full-length receptors. These observations underscore the limitations of studying RTK TM domains in isolation, outside the context of full-length RTKs. Indeed, NMR studies of isolated RTK TM domains in detergent have revealed that the TM domains can form trimers, which are likely irrelevant in biological context [72].

In this work we also sought to measure the effect of ligand binding on RTK dimer stability. It is known that bound ligands stabilize RTK dimers, but the exact contribution of ligand binding to RTK dimer stability has not been measured. Usually the stabilities of the ligand-bound RTK dimers are too high, precluding calculations of the dissociation constant, as also demonstrated here for the three full-length Trk receptors. Since the deletion of the kinase domains decreased the stabilities of the Trk dimers, however, the dissociation constants became measurable for the ligand-bound truncated ECTM Trk dimers. We were thus able to show that the contributions of the three ligands to Trk dimer stability varies from ~-1.5 to ~-2.5 kcal/mole, at 380 nM ligand. To the best of our knowledge, this is the first direct measurement of the energetics behind RTK dimer stabilization by a ligand.

Along with dimer stabilities, we quantified the Intrinsic FRET for all studied Trk dimers, both in the absence and presence of their cognate ligands. Intrinsic FRET is a structural parameter that depends on the distance between the fluorescent proteins and on their relative orientation, but does not depend on dimer stability. We used Intrinsic FRET to follow structural changes that occur on the cytoplasmic side of the receptor upon ligand binding to the extracellular domains. We characterized full-length constructs, where the fluorescent proteins were attached to the C-termini of the receptors via flexible, 15-residue $(GGS)_5$ linkers. We also characterized truncated ECTM Trk constructs, in which the fluorescent proteins were attached to the TM domains via flexible, 15-residue $(GGS)_5$ linkers.

We observed that the Intrinsic FRET value for full-length Trk-C changes upon ligand binding (Table 3-1). Since the fluorescent proteins are attached to the C-termini via flexible linkers, the measured change is indicative of a change in the relative positioning of the C-termini in response to ligand. We further observed that the Intrinsic FRET for ECTM Trk-A and Trk-B

changes upon ligand binding. Since in this case the fluorescent proteins are attached to the C-termini of the TM domains via flexible linkers, differences in Intrinsic FRET are indicative of changes in the relative positioning of the TM C-termini upon ligand binding.

The linkers used to attach the fluorescent proteins to the Trk receptors have been shown previously to behave as random coils [59]. If the orientation of the fluorescent proteins at the end of the linkers is random, the Intrinsic FRET will depend primarily on the distance between the fluorescent proteins in the Trk dimers, as shown in equation 13. In Tables 3-1 and 3-2, we calculate the distances between the fluorescent proteins under the assumption of random orientation of the fluorophores, an assumption which may not be entirely correct. Even if the exact distances are not precisely accurate, the relative changes in fluorescent protein separation due to ligand binding should still hold true. These distances allow for visualization of the conformational changes that occur in response to ligand binding to the Trk receptors.

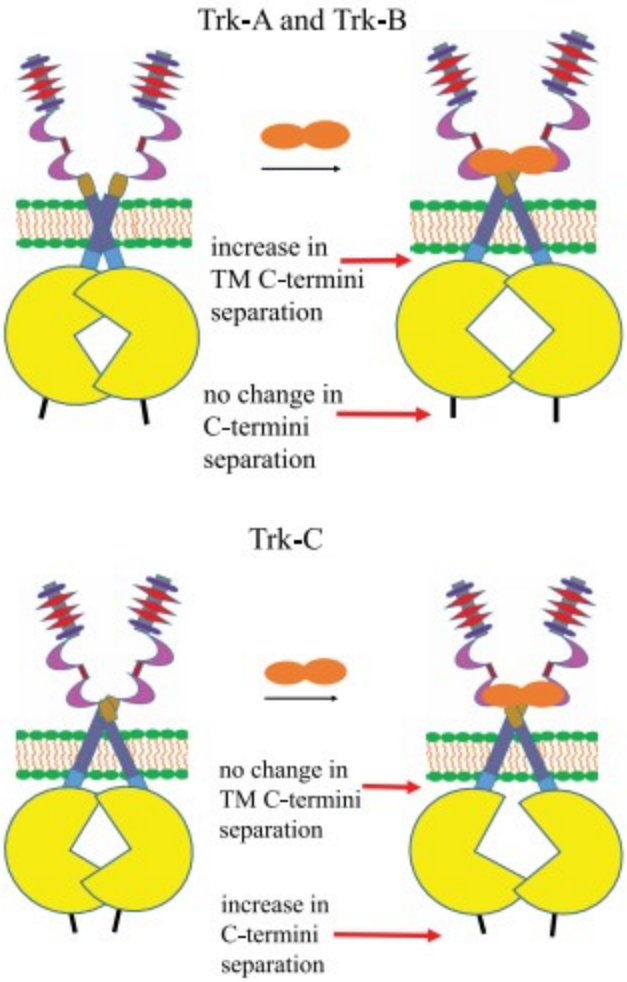

Figure 3-7. The three Trk receptors undergo conformational changes in the IC region after their cognate ligands bind to their extracellular domains. Top: Schematic depiction of the changes occurring in Trk-A and Trk-B. The TM domain C-termini move apart upon ligand binding, while the distance between the C-termini of the receptors does not change in a significant way. Bottom: Schematic depiction of the changes occurring in Trk-C in response to ligand binding. The C-termini move apart upon ligand binding, but the average distance between the TM domain C-termini does not change in a significant way.

A cartoon illustrating the change in these distances is shown in Figure 3-7. In the top panel we depict the changes occurring in Trk-A and Trk-B in response to ligand binding. We show that the TM domain C-termini move apart upon ligand binding, while the distances between the C-termini of the receptors do not change in a significant way. This implies conformational changes in the Trk-A and Trk-B IC domain dimers upon ligand binding. In the bottom panel, we depict the Trk-C case, where the average distance between the TM domain C-termini does not change in a significant way, but the C-termini move further apart. This also implies conformational changes in the Trk-C IC domain dimer upon h-NT-3 binding. While the nature of the ligand-induced changes are different in the cases of Trk-A and Trk-B, on one hand, and Trk-C, on the other, the data suggest that all three Trk receptors undergo conformational changes in the IC region after their cognate ligands bind to their extracellular domains. These changes are likely critical for signal propagation across the plasma membrane.

3-4: Implications

Two RTK activation models have been widely discussed in the literature: (1) the "diffusion-based" or or "canonical" model , which postulates that RTKs dimerize and activate each other only upon ligand binding (but have no propensity to interact with each other and are always monomeric in the absence of ligand [1],[5], and (2) the "pre-formed dimer model," in which RTKs form constitutive dimers, which get activated in response to ligand binding [6][11][20][56][12]**.** However, quantitative measurements of dimerization, such as the ones described here, reconcile these seemingly contradictory models. Indeed, here we find that the measured dissociation constants vary for the different Trk receptors, even though they belong to the same receptor family. Depending on the exact value of the two-dimensional dissociation constant and the expression

levels, RTKs may appear to be predominantly monomeric or predominantly dimeric at a specific expression level, in accordance with the law of mass action.

An important role of the ligand in the pre-formed dimer model is to induce a structural change in the RTK dimer that reorients the catalytic domains for efficient activation [73][12][13][17][18]. However, this role has been recently challenged because the linkage between the different RTK domains has been proposed to be flexible [24]. If this is the case, the different domains are not structurally coupled, and thus structural information cannot be propagated along the length of an RTK. Resolving this controversy is challenging, as there are experimental limitations in following conformational changes in the intracellular domains of RTK dimers upon ligand binding to their EC domains, especially in the context of the full length receptors in the plasma membrane of live cells. Here, we provide evidence of conformational changes in the intracellular portions of the Trk dimers through measurements of Intrinsic FRET. The observed structural change ensures that the kinase domains adopt a signaling-competent orientation only upon ligand binding and can explain how RTKs which form very strong preformed dimers, such as Trk-B, can be activated by their ligands.

Overall, this work supports a model of Trk activation in which (1) Trks have a propensity to interact laterally and to form dimers even in the absence of ligand, (2) different unliganded Trk dimers have different stabilities (and thus different dimer abundance at physiological concentrations), (3) ligand binding leads to Trk dimer stabilization and (4) ligand binding induces a structural changes in the Trk dimer. Thus, an increase in the expression level can cause a transition from predominantly monomeric to predominantly dimeric populations, even in the absence of ligand. When ligand binds to the unliganded dimers, it induces a transition to a

structurally distinct dimeric state with higher stability. This model views RTK activation through the lens of physical chemistry and we term it the "transition model of RTK activation."

It is tempting to speculate that all of the 58 RTKs follow the transition model of RTK activation. Alternatively, it is possible that no single model can capture the activation mechanism of all 58 RTKs. If this is the case, then the activation mechanism needs to be elucidated experimentally for every one of the 58 RTKs. The quantitative FRET methodology used in this work can help in this pursuit of basic knowledge about RTK activation.

3-5: Author contributions: F.A. performed all experiments. F.A. and K.H. analyzed the data and wrote the paper.

3-6: Acknowledgements: Supported by NIH GM068619. We thank Janet Aiyedun for help with data analysis, Michael Paul for reading the manuscript prior to publication, and Dr. Christopher King for the development of the data acquisition and analysis software.

3-7: References

[1] J. Schlessinger, "Cell signaling by receptor tyrosine kinases.," *Cell*, vol. 103, no. 2, pp. 211–25, Oct. 2000.

[2] E. Li and K. Hristova, "Role of receptor tyrosine kinase transmembrane domains in cell signaling and human pathologies.," *Biochemistry*, vol. 45, no. 20, pp. 6241–51, May 2006.

[3] A. Weiss and J. Schlessinger, "Switching signals on or off by receptor dimerization.," *Cell*, vol. 94, no. 3, pp. 277–80, Aug. 1998.

[4] E. B. Pasquale, "Eph receptors and ephrins in cancer: bidirectional signalling and beyond.," *Nat. Rev. Cancer*, vol. 10, no. 3, pp. 165–80, Mar. 2010.

[5] W. J. Fantl, D. E. Johnson, and L. T. Williams, "Signalling by receptor tyrosine kinases.," *Annu. Rev. Biochem.*, vol. 62, pp. 453–81, 1993.

[6] C.-C. Lin *et al.*, "Inhibition of basal FGF receptor signaling by dimeric Grb2.," *Cell*, vol. 149, no. 7, pp. 1514–24, Jun. 2012.

[7] M. A. Lemmon and J. Schlessinger, "Cell signaling by receptor tyrosine kinases.," *Cell*, vol. 141, no. 7, pp. 1117–34, Jun. 2010.

[8] M. A. Lemmon, J. Schlessinger, and K. M. Ferguson, "The EGFR family: not so prototypical receptor tyrosine kinases.," *Cold Spring Harb. Perspect. Biol.*, vol. 6, no. 4, p. a020768, Apr. 2014.

[9] J. Schlessinger, "Receptor tyrosine kinases: legacy of the first two decades.," *Cold Spring Harb. Perspect. Biol.*, vol. 6, no. 3, Mar. 2014.

[10] J. Schlessinger and M. A. Lemmon, "SH2 and PTB domains in tyrosine kinase

signaling.," *Sci. STKE*, vol. 2003, no. 191, p. RE12, Jul. 2003.

[11] C. C. Valley, A. K. Lewis, and J. N. Sachs, "Piecing it together: Unraveling the elusive structure-function relationship in single-pass membrane receptors.," *Biochim. Biophys. acta. Biomembr.*, vol. 1859, no. 9 Pt A, pp. 1398–1416, Sep. 2017.

[12] T. Moriki, H. Maruyama, and I. N. Maruyama, "Activation of preformed EGF receptor dimers by ligand-induced rotation of the transmembrane domain.," *J. Mol. Biol.*, vol. 311, no. 5, pp. 1011–26, Aug. 2001.

[13] N. F. Endres *et al.*, "Conformational coupling across the plasma membrane in activation of the EGF receptor.," *Cell*, vol. 152, no. 3, pp. 543–56, Jan. 2013.

[14] S. J. Fleishman, J. Schlessinger, and N. Ben-Tal, "A putative molecular-activation switch in the transmembrane domain of erbB2.," *Proc. Natl. Acad. Sci. U. S. A.*, vol. 99, no. 25, pp. 15937–40, Dec. 2002.

[15] E. V Bocharov *et al.*, "Left-handed dimer of EphA2 transmembrane domain: Helix packing diversity among receptor tyrosine kinases.," *Biophys. J.*, vol. 98, no. 5, pp. 881–9, Mar. 2010.

[16] E. V Bocharov, D. M. Lesovoy, S. A. Goncharuk, M. V Goncharuk, K. Hristova, and A. S. Arseniev, "Structure of FGFR3 transmembrane domain dimer: implications for signaling and human pathologies.," *Structure*, vol. 21, no. 11, pp. 2087–93, Nov. 2013.

[17] S. Sarabipour and K. Hristova, "Mechanism of FGF receptor dimerization and activation.," *Nat. Commun.*, vol. 7, p. 10262, Jan. 2016.

[18] S. Sarabipour, K. Ballmer-Hofer, and K. Hristova, "VEGFR-2 conformational switch in response to ligand binding.," *Elife*, vol. 5, p. e13876, Apr. 2016.

[19] C. A. Bell, J. A. Tynan, K. C. Hart, A. N. Meyer, S. C. Robertson, and D. J. Donoghue, "Rotational coupling of the transmembrane and kinase domains of the Neu receptor tyrosine kinase.," *Mol. Biol. Cell*, vol. 11, no. 10, pp. 3589–99, Oct. 2000.

[20] E. V Bocharov, G. V Sharonov, O. V Bocharova, and K. V Pavlov, "Conformational transitions and interactions underlying the function of membrane embedded receptor protein kinases.," *Biochim. Biophys. acta. Biomembr.*, vol. 1859, no. 9 Pt A, pp. 1417–1429, Sep. 2017.

[21] C. Lu, L.-Z. Mi, T. Schürpf, T. Walz, and T. A. Springer, "Mechanisms for kinase-mediated dimerization of the epidermal growth factor receptor.," *J. Biol. Chem.*, vol. 287, no. 45, pp. 38244–53, Nov. 2012.

[22] C. Lu *et al.*, "Structural evidence for loose linkage between ligand binding and kinase activation in the epidermal growth factor receptor.," *Mol. Cell. Biol.*, vol. 30, no. 22, pp. 5432–43, Nov. 2010.

[23] A. Sorokin, "Activation of the EGF receptor by insertional mutations in its juxtamembrane regions.," *Oncogene*, vol. 11, no. 8, pp. 1531–40, Oct. 1995.

[24] D. M. Freed *et al.*, "EGFR Ligands Differentially Stabilize Receptor Dimers to Specify Signaling Kinetics.," *Cell*, vol. 171, no. 3, p. 683–695.e18, Oct. 2017.

[25] R. Kuruvilla *et al.*, "A neurotrophin signaling cascade coordinates sympathetic neuron development through differential control of TrkA trafficking and retrograde signaling.," *Cell*, vol. 118, no. 2, pp. 243–55, Jul. 2004.

[26] M. Ascaño, A. Richmond, P. Borden, and R. Kuruvilla, "Axonal targeting of Trk receptors via transcytosis regulates sensitivity to neurotrophin responses.," *J. Neurosci.*,

vol. 29, no. 37, pp. 11674–85, Sep. 2009.

[27] J. Houtz, P. Borden, A. Ceasrine, L. Minichiello, and R. Kuruvilla, "Neurotrophin Signaling Is Required for Glucose-Induced Insulin Secretion.," *Dev. Cell*, vol. 39, no. 3, pp. 329–345, 2016.

[28] T. Sasahira *et al.*, "Trks are novel oncogenes involved in the induction of neovascularization, tumor progression, and nodal metastasis in oral squamous cell carcinoma.," *Clin. Exp. Metastasis*, vol. 30, no. 2, pp. 165–76, Feb. 2013.

[29] V. K. Gupta, Y. You, V. B. Gupta, A. Klistorner, and S. L. Graham, "TrkB receptor signalling: implications in neurodegenerative, psychiatric and proliferative disorders.," *Int. J. Mol. Sci.*, vol. 14, no. 5, pp. 10122–42, May 2013.

[30] H. Hondermarck, "Neurotrophins and their receptors in breast cancer.," *Cytokine Growth Factor Rev.*, vol. 23, no. 6, pp. 357–65, Dec. 2012.

[31] M. Bothwell, "Recent advances in understanding neurotrophin signaling.," *F1000Research*, vol. 5, 2016.

[32] P. K. Tan *et al.*, "Monitoring interactions between receptor tyrosine kinases and their downstream effector proteins in living cells using bioluminescence resonance energy transfer.," *Mol. Pharmacol.*, vol. 72, no. 6, pp. 1440–6, Dec. 2007.

[33] A. B. Keeler, D. Suo, J. Park, and C. D. Deppmann, "Delineating neurotrophin-3 dependent signaling pathways underlying sympathetic axon growth along intermediate targets.," *Mol. Cell. Neurosci.*, vol. 82, pp. 66–75, 2017.

[34] D. J. Belliveau *et al.*, "NGF and neurotrophin-3 both activate TrkA on sympathetic neurons but differentially regulate survival and neuritogenesis.," *J. Cell Biol.*, vol. 136, no.

2, pp. 375–88, Jan. 1997.

[35] D. Bodmer, M. Ascaño, and R. Kuruvilla, “Isoform-specific dephosphorylation of dynamin1 by calcineurin couples neurotrophin receptor endocytosis to axonal growth.,” *Neuron*, vol. 70, no. 6, pp. 1085–99, Jun. 2011.

[36] L. Chen, J. Placone, L. Novicky, and K. Hristova, “The extracellular domain of fibroblast growth factor receptor 3 inhibits ligand-independent dimerization.,” *Sci. Signal.*, vol. 3, no. 150, p. ra86, Nov. 2010.

[37] L. Chen, L. Novicky, M. Merzlyakov, T. Hristov, and K. Hristova, “Measuring the energetics of membrane protein dimerization in mammalian membranes.,” *J. Am. Chem. Soc.*, vol. 132, no. 10, pp. 3628–35, Mar. 2010.

[38] S. Sarabipour, N. Del Piccolo, and K. Hristova, “Characterization of membrane protein interactions in plasma membrane derived vesicles with quantitative imaging Förster resonance energy transfer.,” *Acc. Chem. Res.*, vol. 48, no. 8, pp. 2262–9, Aug. 2015.

[39] C. King, M. Stoneman, V. Raicu, and K. Hristova, “Fully quantified spectral imaging reveals in vivo membrane protein interactions.,” *Integr. Biol. (Camb).*, vol. 8, no. 2, pp. 216–29, Feb. 2016.

[40] G. Biener *et al.*, “Development and experimental testing of an optical micro-spectroscopic technique incorporating true line-scan excitation.,” *Int. J. Mol. Sci.*, vol. 15, no. 1, pp. 261–76, Dec. 2013.

[41] J. Adler, A. I. Shevchuk, P. Novak, Y. E. Korchev, and I. Parmryd, “Plasma membrane topography and interpretation of single-particle tracks.,” *Nat. Methods*, vol. 7, no. 3, pp. 170–1, Mar. 2010.

[42] I. Parmryd and B. Onfelt, “Consequences of membrane topography.,” *FEBS J.*, vol. 280, no. 12, pp. 2775–84, Jun. 2013.

[43] C. King, S. Sarabipour, P. Byrne, D. J. Leahy, and K. Hristova, “The FRET signatures of noninteracting proteins in membranes: simulations and experiments.,” *Biophys. J.*, vol. 106, no. 6, pp. 1309–17, Mar. 2014.

[44] B. Sinha *et al.*, “Cells respond to mechanical stress by rapid disassembly of caveolae.,” *Cell*, vol. 144, no. 3, pp. 402–13, Feb. 2011.

[45] D. R. Singh, F. Ahmed, S. Sarabipour, and K. Hristova, “Intracellular Domain Contacts Contribute to Ecadherin Constitutive Dimerization in the Plasma Membrane.,” *J. Mol. Biol.*, vol. 429, no. 14, pp. 2231–2245, 2017.

[46] D. R. Singh *et al.*, “Unliganded EphA3 dimerization promoted by the SAM domain.,” *Biochem. J.*, vol. 471, no. 1, pp. 101–9, Oct. 2015.

[47] D. R. Singh *et al.*, “EphA2 Receptor Unliganded Dimers Suppress EphA2 Pro-tumorigenic Signaling.,” *J. Biol. Chem.*, vol. 290, no. 45, pp. 27271–9, Nov. 2015.

[48] H. Yano, F. Cong, R. B. Birge, S. P. Goff, and M. V Chao, “Association of the Abl tyrosine kinase with the Trk nerve growth factor receptor.,” *J. Neurosci. Res.*, vol. 59, no. 3, pp. 356–64, Feb. 2000.

[49] C. King, D. Wirth, S. Workman, and K. Hristova, “Cooperative interactions between VEGFR2 extracellular Ig-like subdomains ensure VEGFR2 dimerization.,” *Biochim. Biophys. acta. Gen. Subj.*, vol. 1861, no. 11 Pt A, pp. 2559–2567, Nov. 2017.

[50] D. R. Singh, P. Kanvinde, C. King, E. B. Pasquale, and K. Hristova, “The EphA2 receptor is activated through induction of distinct, ligand-dependent oligomeric structures.,”

Commun. Biol., vol. 1, p. 15, 2018.

[51] B. D. Adair and D. M. Engelman, "Glycophorin A helical transmembrane domains dimerize in phospholipid bilayers: a resonance energy transfer study.," *Biochemistry*, vol. 33, no. 18, pp. 5539–44, May 1994.

[52] M. Li, L. G. Reddy, R. Bennett, N. D. Silva, L. R. Jones, and D. D. Thomas, "A fluorescence energy transfer method for analyzing protein oligomeric structure: application to phospholamban.," *Biophys. J.*, vol. 76, no. 5, pp. 2587–99, May 1999.

[53] S. Schick, L. Chen, E. Li, J. Lin, I. Köper, and K. Hristova, "Assembly of the m2 tetramer is strongly modulated by lipid chain length.," *Biophys. J.*, vol. 99, no. 6, pp. 1810–7, Sep. 2010.

[54] D. Martin-Zanca, R. Oskam, G. Mitra, T. Copeland, and M. Barbacid, "Molecular and biochemical characterization of the human trk proto-oncogene.," *Mol. Cell. Biol.*, vol. 9, no. 1, pp. 24–33, Jan. 1989.

[55] J. Jullien, V. Guili, L. F. Reichardt, and B. B. Rudkin, "Molecular kinetics of nerve growth factor receptor trafficking and activation.," *J. Biol. Chem.*, vol. 277, no. 41, pp. 38700–8, Oct. 2002.

[56] J. Shen and I. N. Maruyama, "Nerve growth factor receptor TrkA exists as a preformed, yet inactive, dimer in living cells.," *FEBS Lett.*, vol. 585, no. 2, pp. 295–9, Jan. 2011.

[57] P. K. Wolber and B. S. Hudson, "An analytic solution to the Förster energy transfer problem in two dimensions.," *Biophys. J.*, vol. 28, no. 2, pp. 197–210, Nov. 1979.

[58] C. King, V. Raicu, and K. Hristova, "Understanding the FRET Signatures of Interacting Membrane Proteins.," *J. Biol. Chem.*, vol. 292, no. 13, pp. 5291–5310, Mar. 2017.

[59] T. H. Evers, E. M. W. M. van Dongen, A. C. Faesen, E. W. Meijer, and M. Merkx, "Quantitative understanding of the energy transfer between fluorescent proteins connected via flexible peptide linkers.," *Biochemistry*, vol. 45, no. 44, pp. 13183–92, Nov. 2006.

[60] S. Sarabipour and K. Hristova, "FGFR3 unliganded dimer stabilization by the juxtamembrane domain.," *J. Mol. Biol.*, vol. 427, no. 8, pp. 1705–14, Apr. 2015.

[61] R. T. Uren and A. M. Turnley, "Regulation of neurotrophin receptor (Trk) signaling: suppressor of cytokine signaling 2 (SOCS2) is a new player.," *Front. Mol. Neurosci.*, vol. 7, p. 39, 2014.

[62] D. Soppet *et al.*, "The neurotrophic factors brain-derived neurotrophic factor and neurotrophin-3 are ligands for the trkB tyrosine kinase receptor.," *Cell*, vol. 65, no. 5, pp. 895–903, May 1991.

[63] A. Rodríguez-Tébar, G. Dechant, R. Götz, and Y. A. Barde, "Binding of neurotrophin-3 to its neuronal receptors and interactions with nerve growth factor and brain-derived neurotrophic factor.," *EMBO J.*, vol. 11, no. 3, pp. 917–22, Mar. 1992.

[64] R. Urfer, P. Tsoulfas, L. O'Connell, and L. G. Presta, "Specificity determinants in neurotrophin-3 and design of nerve growth factor-based trkC agonists by changing central beta-strand bundle residues to their neurotrophin-3 analogs.," *Biochemistry*, vol. 36, no. 16, pp. 4775–81, Apr. 1997.

[65] R. Urfer, P. Tsoulfas, D. Soppet, E. Escandón, L. F. Parada, and L. G. Presta, "The binding epitopes of neurotrophin-3 to its receptors trkC and gp75 and the design of a multifunctional human neurotrophin.," *EMBO J.*, vol. 13, no. 24, pp. 5896–909, Dec. 1994.

[66] L. Ivanisevic, W. Zheng, S. B. Woo, K. E. Neet, and H. U. Saragovi, "TrkA receptor 'hot spots' for binding of NT-3 as a heterologous ligand.," *J. Biol. Chem.*, vol. 282, no. 23, pp. 16754–63, Jun. 2007.

[67] S. Sarabipour and K. Hristova, "Pathogenic Cysteine Removal Mutations in FGFR Extracellular Domains Stabilize Receptor Dimers and Perturb the TM Dimer Structure.," *J. Mol. Biol.*, vol. 428, no. 20, pp. 3903–3910, 2016.

[68] J. Shen and I. N. Maruyama, "Brain-derived neurotrophic factor receptor TrkB exists as a preformed dimer in living cells.," *J. Mol. Signal.*, vol. 7, no. 1, p. 2, Jan. 2012.

[69] P. S. Mischel, J. A. Umbach, S. Eskandari, S. G. Smith, C. B. Gundersen, and G. A. Zampighi, "Nerve growth factor signals via preexisting TrkA receptor oligomers.," *Biophys. J.*, vol. 83, no. 2, pp. 968–76, Aug. 2002.

[70] D. O. Clary, G. Weskamp, L. R. Austin, and L. F. Reichardt, "TrkA cross-linking mimics neuronal responses to nerve growth factor.," *Mol. Biol. Cell*, vol. 5, no. 5, pp. 549–63, May 1994.

[71] T. Wehrman, X. He, B. Raab, A. Dukipatti, H. Blau, and K. C. Garcia, "Structural and mechanistic insights into nerve growth factor interactions with the TrkA and p75 receptors.," *Neuron*, vol. 53, no. 1, pp. 25–38, Jan. 2007.

[72] S. Manni *et al.*, "Structural and functional characterization of alternative transmembrane domain conformations in VEGF receptor 2 activation.," *Structure*, vol. 22, no. 8, pp. 1077–1089, Aug. 2014.

Chapter 4: The molecular basis of receptor tyrosine kinase ligand functional selectivity: A Trk-B case study

4-1: Introduction

Receptors in the plasma membrane can bind multiple ligands and can initiate multiple downstream signaling cascades that control cellular physiology in health and disease. Recent work has uncovered that different ligands can selectively engage some signaling pathways over others and can lead to different biological outcomes while acting through the same receptor. This phenomenon is known as “ligand bias” or “ligand functional selectivity” and has been extensively characterized for the largest class of membrane receptors, the seven helix G-protein coupled receptors (GPCRs). The mechanism of ligand bias in GPCR signaling is now established: different GPCR ligands stabilize different functional receptor conformations, and each of the conformations triggers efficiently only a subset of the possible downstream signaling cascades. The discovery and the mechanistic studies of GPCR bias have redefined fundamental concepts in pharmacology, and have opened up new possibilities for the development of more effective and specific therapeutics.

While most ligand bias investigations have focused on the GPCRs, ligand bias has also been observed for the second largest class of membrane receptors, the receptor tyrosine kinases (RTKs). RTKs are single-pass transmembrane proteins that control cell growth, differentiation, motility, and metabolism [1][2], by transducing biochemical signals via lateral dimerization or oligomerization in the plasma membrane. Their N-terminal extracellular (EC) regions, composed of characteristic arrays of structural domains, bind the activating ligands [3]. They have single transmembrane helices and intracellular kinase domains (Fig. 1). The cross-phosphorylation of

two kinase domains in the ligand-bound dimers and oligomers stimulates catalytic activity, which results in the phosphorylation of cytoplasmic substrates, ultimately activating signaling cascades that control cell behavior [2][4][5].

It is now well documented that different ligands can induce different biological responses when binding and activating the same RTK [6][7][8][9][10][11][12][13][14]. There are reports of ligand bias involving the ERBB receptors [15], the fibroblast growth factor receptors (FGFRs) [7], and the Eph receptors[16]. However, the mechanism behind this ligand bias is not well understood for the RTKs, and is a subject of debate. Some studies have proposed that RTK ligand bias occurs through a mechanism that is analogous to the one used by the GPCRs, i.e. different RTK ligands stabilize different RTK dimer configurations, leading to differential kinase domains activity. Others, however, argue that the mechanism is fundamentally different, as RTK kinase domains cannot sense the identity of the bound ligand because the linkers between the different RTK domains are flexible. Rather, these researchers propose that the stability of the RTK dimer is the important parameter that controls ligand bias.

Here we investigate the biophysical basis behind biased signaling by TrkB, an RTK that belongs to the three member Tropomyosin receptor kinases (Trks) family. This family is characterized by extracellular domains that contain three tandem leucine rich repeats flanked by cysteine rich domains and two immunoglobulin-like domains [17][18]. The signaling cascades initiated by the Trk receptors control neuronal cell survival and proliferation, axonal and dendritic growth, as well as synaptic connections and synaptic plasticity [19][20][21][22][23][24]. Trk-B, studied here, plays a vital role in neural plasticity in early CNS development and in adulthood [25][18]. It is also present in non-neuronal cells such as glia and Schwann cells [26][27][28].

Trk-B signals in response to three different neurotrophins, h-BDNF, h-NT-3 and h-NT-4, which are small biological molecules with 50% sequence identity [29]. These neurotrophins play crucial role in the development, maintenance, and survival of neurons in both the peripheral and central nervous system [29][30]. Their binding to Trk-B leads to TrkB cross-phosphorylation and activation of downstream signaling. The main downstream signaling effectors which are activated by Trk-B are Ras mitogen activated protein kinase (MAPK), phosphotidylinositol 3-kinase (P13K), Akt, and PLCγ–Ca2 [31] .

The three neurotrophins, ligands, h-BDNF, h-NT-3 and h-NT-4, have been reported to have similar binding affinities for Trk-B. There are also reports of similar Trk-B phosphorylation and activation in response to these ligands. Yet, these three neurotrophins can lead to different cellular responses when signaling through Trk-B. H-BDNF has been shown to play a much more profound role than h-NT-4 in synaptic transmission, plasticity, and in higher cognitive functions [32][33][25][34][35][36][37][38]. On the other hand, h-NT-4 is more potent at inducing neuronal survival and synaptic maturation [38][39]. In NIH3T3 cells, both h-BDNF and h-NT-4 are more potent than h-NT-3 in initiating growth responses [40][41].

What factors could underlie the differential responses of Trk-B to the three neurotrophins? By analogy to the GPCRs, it can be expected that ligand bias starts with events at the plasma membrane. It can be expected that either differences in the conformation of the kinase domains in response to the different ligands, or the stability of the ligand-bound dimers, or both, may be responsible. The conformations and the stabilities of the different neurotrophin-bound Trk-B dimers have not been compared, however.

In order to study protein interactions in the plasma membrane in quantitative terms, we have previously established a FRET-based assay that can yield RTK association constants and

can report on the occurrence of conformational changes upon ligand binding. Using this assay, we have previously shown that Trk-B forms a very stable dimer (K_{diss} = 12 ± 2 rec/□m^2(Chapter 3)), even in the absence of ligand. The binding of h-BDNF to the pre-formed Trk-B dimer triggers a conformational change in the dimer and further enhances its stability. Here we investigate the response of Trk-B to h-NT-3 and h-NT-4, in order to compare it to the response to h-BDNF and thus gain insight into ligand functional selectivity.

4-2: Results

Here we use FRET to characterize the lateral interactions between Trk-B receptors, which are labeled with fluorescent proteins at the C-terminus (either mTurquoise or YFP, a FRET pair) via flexible $(GGS)_5$ linkers, in the presence of two ligands, h-NT-3 and h-NT-4. The cloning of the plasmids encoding for these constructs, and the FRET-based assessment of Trk-B interactions in the absence of ligand and in the presence of h-BDNF has been described in chapter 2 and chapter 3.

Experiments were conducted in the presence of 5μg/mL (380nM) h-NT-3 or h-NT-4 using the FSI-FRET method. The used ligand concentration is well above the reported ligand-receptor dissociation constants, which are in the pM to low nM range [28][41][42][43][33]. The FSI-FRET method, briefly described in chapter 2, yields three parameters: FRET efficiency, donor (Trk-B-mTurquoise) concentration, and acceptor (Trk-B-YFP) concentration, in small patches of the plasma membrane of live cells. Hundreds of individual cells, all expressing different amounts of Trk-B- mTurquoise and Trk-B-YFP, are analyzed and combined to produce binding curves.

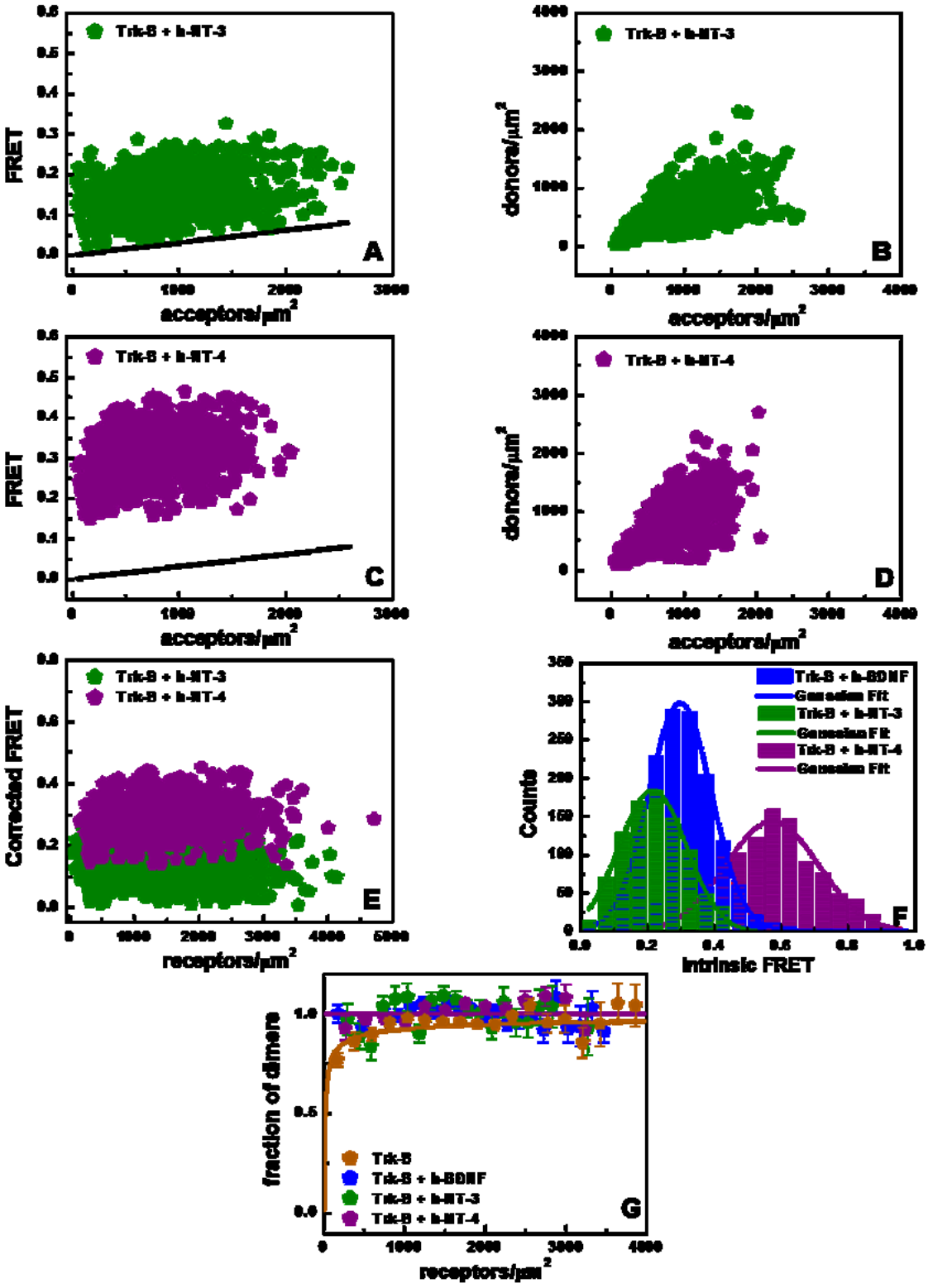
Trk-B + h-NT-3
FRET
acceptors/μm²
A
donors/μm²
B
Trk-B + h-NT-4
C
D
Corrected FRET
receptors/μm²
E
Trk-B + h-BDNF
Gaussian Fit
Counts
Intrinsic FRET
F
fraction of dimers
Trk-B
G

Figure 4- 1: Comparison of FRET data for Trk-B in the presence of two ligands: h-NT-3 and h-NT-4. A and C: FRET data as a function of acceptor concentration. The solid black line is the "proximity" FRET. B and D: donor vs. acceptor concentration for both ligands. E: proximity-corrected FRET as a function of total Trk-B concentration. F: histograms of Trk-B FRET data in the presence h-BDNF, h-NT-3, and h-NT-4. G: dimerization curves for Trk-B in the absence and presence of ligands as a function of Trk-B concentration.

Figures 4-1-A and 4-1-C show the FRET efficiencies in single cells as a function of the acceptor concentration in the presence of h-NT-3, and h-NT-4, respectively, while Figures 4-1-B and 4-1-D shows the donor concentration as a function of the acceptor concentration in the presence of the two ligands. In Figures 4-1-A and 4-1-C we also include the so-called "proximity" FRET which occurs due to the random close approach (within 100 Å) of the donors and acceptors confined to the two-dimensional plasma membrane. The solid lines Figures in 4-1-A and 4-1-C show the best-fit proximity contributions, determined as described in chapter 2. The measured FRET is corrected for this "proximity" contribution following an established protocol [44][45][46] to obtain FRET due to specific Trk-B interactions, shown in Figure 4-1-E as a function of the total concentration. We see that the corrected FRET does not depend on the concentration, which indicates that Trk-B is constitutively dimeric over the concentration range that is accessible in our experiments. In this case the measured FRET in each cell region is proportional to the value of Intrinsic FRET (Ẽ, see equation 11), a structural parameter which depends on the positioning and dynamics of the fluorescent proteins attached to the C-termini of the receptors [47]. The histograms of Intrinsic FRET values, measured in the different cells for each receptor/ligand pair, are shown in Figure 4-1-F. Also included in Figure 4-1-E are previously measured Intrinsic FRET values for Trk-B in the presence of 380 nM h-BDNF. The three histograms are fit to Gaussian functions, and the mean and standard errors are shown in Table 4-1. Figure 4-1-E shows the binned dimeric fractions in the presence of the three ligands, as well as the dimeric fraction measured previously in the absence of ligand for Trk-B. Notably, Trk-B forms a very stable dimer even in the absence of ligand (dimerization parameters shown in Table 4-1).

Full length	K_{diss}(rec/μm²)	ΔG (kcal/mol)	Intrinsic FRET (Ẽ)	d(Å)
Trk-B	12 ± 2	-6.72 ± 0.10	0.35 ± 0.04	60 ± 2
Trk-B+ h-BDNF	100% dimer	n.d.	0.30 ± 0.02	63 ± 1
Trk-B+ h-NT-3	100% dimer	n.d.	0.22 ± 0.02	67 ± 1
Trk-B+ h-NT-4	100% dimer	n.d.	0.57 ± 0.02	52 ± 1

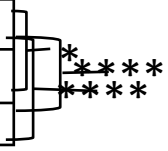

Table 4- 1: Comparing dimerization parameters for full length Trk-B receptor in the presence of three ligands (n.s. not statistically significant; *p-value between 0.05 and 0.01; ****p-Value <0.0001).

Taken together, the measured Intrinsic FRET values in Table 4-1 demonstrate that the distance and/or the orientation of the FPs, attached to the C-terminus of Trk-B, are different when the three different ligands are bound. Note that for all ligands, we are interrogating 100% dimeric receptors (Figure 4-1-E), and thus the only difference in the experiments is the identity of the ligand that is bound to the EC domains. Therefore, the results suggest that the three ligands stabilize dimers with different intracellular domain conformations.

To gain additional insights into the effect of the three ligands on Trk-B dimerization, we performed FRET experiments with a truncated ECTM Trk construct with deleted kinase domains. This construct contains the extracellular and transmembrane domains of Trk-B, a 15 amino acid flexible $(GGS)_5$ linker and the fluorescent proteins.

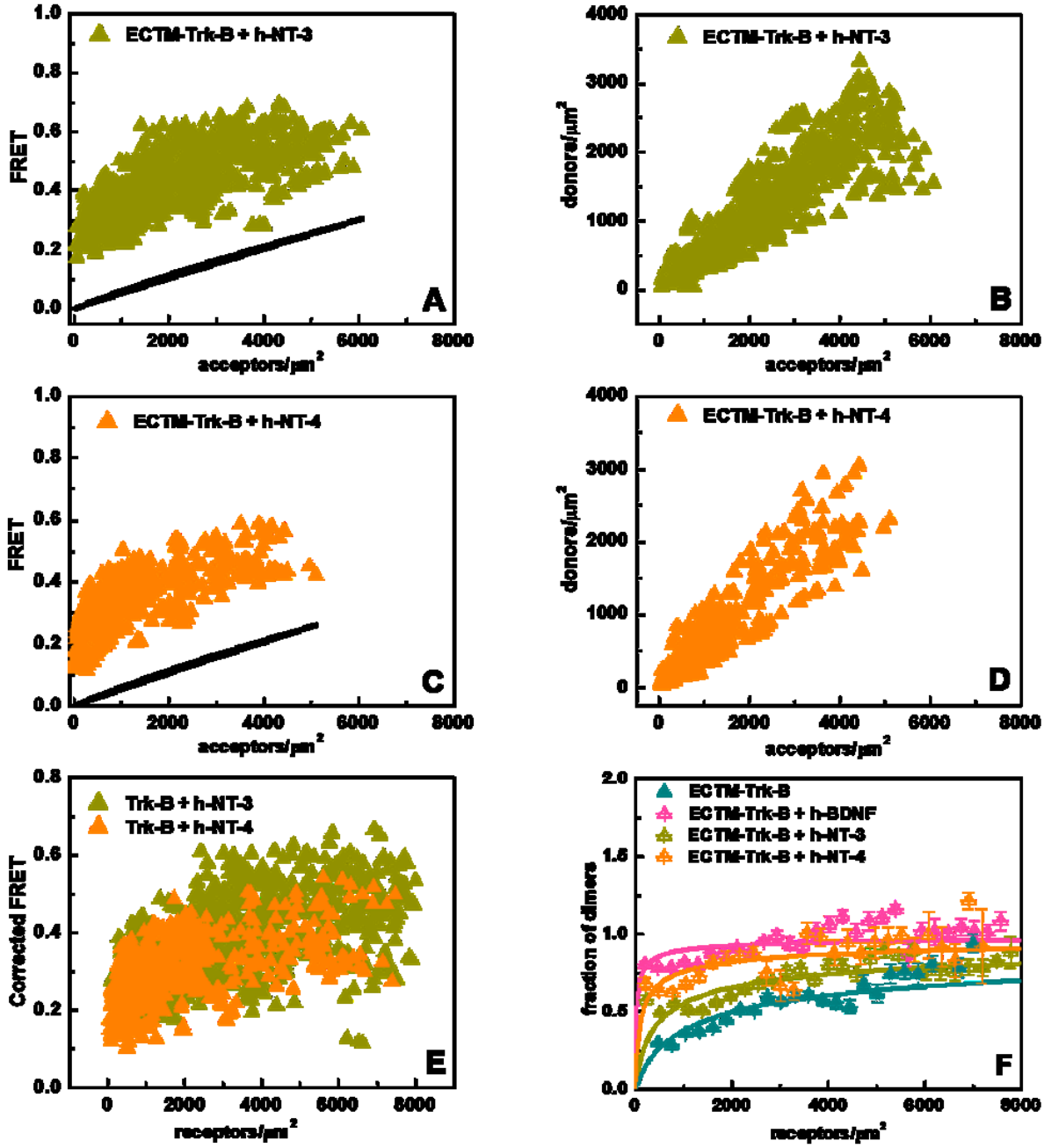

Figure 4- 2: ECTM Trk-B FRET data in the presence of the ligands h-NT-3 and h-NT-4. A and C: FRET as a function of acceptors for hNT-3 and h-NT-4, respectively. The solid black lines indicate the "proximity" FRET in A and C. B and D: plots for donor vs. acceptor concentrations for Trk-A in the presence of h-NT-3 and h-NT-4, respectively. E: proximity-corrected FRET

data for h-NT-3 and h-NT-4. F: Comparison of dimerization curves for Trk-B in the absence and presence of ligands.

In Figure 4-2-A and 4-2-C we show the FRET efficiencies for the ECTM Trk-B construct in the presence of 380 nM of h-NT-3 and h-NT-4, measured for 200-500 individual cells, along with the optimized best-fit proximity FRET contribution. Figure 4-2-B and 4-2-D show the donor concentration versus the acceptor concentration for each of these cells, in the presence of h-NT-3 and h-NT-4. Figure 4-2-E shows the corrected FRET efficiency that is due to specific interactions between the ECTM Trk-B molecules, as a function of the total receptor concentration. Unlike in the case of full-length Trk-B, here the specific FRET increases as a function of the concentration. This indicates that Trk-B monomers and dimers coexist in the plasma membrane, and that the dimer population increases with the concentration as dictated by the law of mass action. A model of monomer-dimer equilibrium from chapter 2, was fitted to the data in Figure 4-2-E. The two unknown parameters in the fit were the dissociation constant, K, a measure of the strength of Trk-B interactions in the presence of 380 nM ligand, and the structural parameter Intrinsic FRET. The best-fit K and Intrinsic FRET values for ECTM Trk-B in the presence of the different ligands are shown in Table 4-2, along with previous results for the ligand h-BDNF. Figure 4-2-F shows experimental binned dimeric fractions in the presence of the three ligands, along with the best-fit. For comparison, we also show the ECTM TrkB dimeric fraction in the absence of ligand.

ECTM	K_{diss} (rec/μm^2)	ΔG (kcal/mol)	Intrinsic FRET (Ẽ)	d(Å)
Trk-B	2018 ± 134	-3.68 ± 0.04	0.82 ± 0.02	42 ± 1
Trk-B+ h-BDNF	23 ± 2	-6.33 ± 0.06	0.50 ± 0.01	55 ± 1
Trk-B+ h-NT-3	710 ± 40	-4.30 ± 0.07	0.85 ± 0.02	41 ± 1
Trk-B+ h-NT-4	150 ± 36	-5.22 ± 0.15	0.68 ± 0.02	48 ± 1

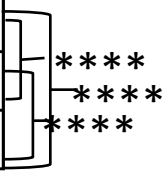

Table 4- 2: Comparison of the dimerization parameters for ECTM-Trk-B construct (****p-Value <0.0001).

.

As seen in Figure 4-2-F and in Table 4-2, the stabilities of the three ligand-bound Trk-B dimers (at 380 nM ligand) are different. Furthermore, the Intrinsic FRET values measured in the presence of the three ligands are different. As the fluorescent proteins are attached to the TM domain C-termini via flexible linkers, these results suggest that the conformations of the Trk-B TM domain dimer are different when different ligands are bound to the EC domain. Thus, both the structures and stabilities of the ligand-bound ECTM Trk-B dimers are different.

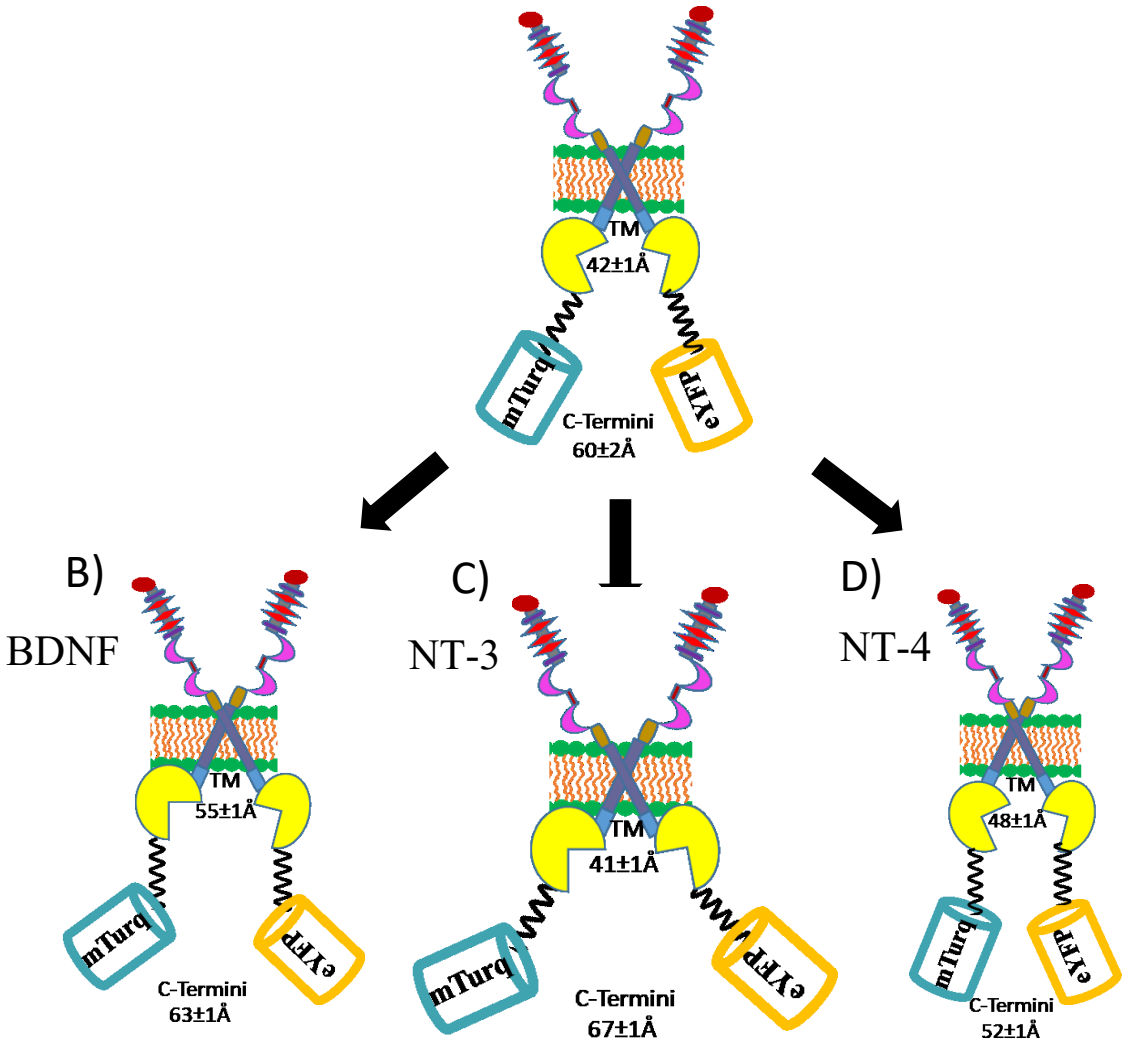

Figure 4- 3: Comparing the conformational differences in the TM and intracellular region of Trk-B in the absence and presence of three ligands: h-BDNF, h-NT-3, and h-NT-4. A: Trk-B in the absence of any ligands. B: Trk-B in the presence of h-BDNF. C: Trk-B in the presence of h-NT-3. D: Trk-B in the presence of h-NT-4. The three different ligands induce three different conformations of Trk-B dimers in the plasma membrane.

In figure 4-3, Cartoon depiction is drawn for Trk-B in the absence and presence of three ligands to demonstrate changes in the conformation of the receptor bound to different ligands. In the presence all three ligands, there are changes in the conformation of Trk-B dimer which occur at the TM and C-termini regions of the receptor, suggestion each ligand is responsible for giving different dimer conformation. The stability of Trk-B dimer is also different for each ligand as reported in Table 4-2, thus, generating different downstream biological responses.

4-3: Discussion

Our understanding of RTK activation has been shaped, to a large degree, by crystal structures of isolated RTK EC domains in the absence and presence of their ligands. Crystal structures of EC domains bound to different activating ligands invariably show some structural differences [48][4][14]. However, it has been unknown if these differences are sensed by the kinase domains of the RTKs to lead to differential signaling outcomes [49][50][51][52].

Two hypotheses have been discussed in the literature to explain the occurrence of RTK ligand bias. According to one hypothesis, ligand bias arises because the conformations of the kinase domain dimers are different when different ligands are bound to the extracellular domains. According to this hypothesis, the conformational changes in the EC domain in response to the bound ligand are transmitted along the length of the RTK and reach the kinase. In support of this view, it has been shown that different ligands, bound to the same RTK, can induce different TM domain dimer conformations, or different conformations of the linker connecting the TM and kinase domains (the so-called JM domain). Yet, there have been no direct demonstrations that the kinase domains can adopt distinct configurations when different ligands are bound to the EC regions. In part, this is due to experimental challenges to assess the conformation of the kinase domains inside cells when different ligands are bound to the EC

domain. Here we overcome the challenges by quantifying the so-called intrinsic FRET between the fluorescent proteins in the Trk-B dimer. We observe differences in Intrinsic FRET in the presence of h-NT-3, h-NT-4, or h-BDNF. These differences in Intrinsic FRET suggest differences in the relative positioning and/or dynamics of the FPs, and of the domains to which the FPs are attached. Therefore, our experiments reveal that the three ligands lead to different Trk-B intracellular configurations, in agreement with this ligand bias hypothesis.

A second, seemingly alternative, hypothesis has been developed, prompted by observations that the EC and IC domains can change conformations independent of each other. Some believe that structural changes in the EC region cannot be propagated to the IC region, presumably because the linkers between the regions are unstructured. This second hypothesis postulates that the differential engagement of downstream molecules in response to different ligands is correlated with the thermodynamic stabilities of the ligand-bound RTK dimers in the plasma membrane. In particular, it has been proposed that RTK dimers with low stability fail to activate all downstream signaling pathways and to engage negative feedback mechanisms. To test if the Trk-B dimer has different stability when bound to h-NT-3, h-NT-4, or h-BDNF, we directly measure and compare the thermodynamic stability of Trk-B dimers at saturating concentrations of h-NT-3, h-NT-4, and h-BDNF. We show that the stability of the ECTM Trk-B dimer is different when the three different ligands are bound. We could not measure thermodynamic stabilities for the full-length ligand-bound Trk-B because they were 100% dimeric in our experiments, due to favorable stabilizing interactions between the kinase domains.

However, we expect that the differences observed for ECTM Trk-B hold true also in the case of full-length Trk-B. Thus, overall our data are consistent with this second hypothesis about ligand bias. There is no reason for the two hypotheses, discussed above, to be mutually

exclusive. In fact, our work demonstrates that they are not. Indeed, we find here that each of the different ligands, h-NT-3, h-NT-4, and h-BDNF, stabilizes Trk-B dimers with different conformations and with different stabilities. Furthermore, structure and stabilities can be expected to be correlated.

This work gives new insights into the general mechanism behind ligand bias. GPCRs transduce biochemical signals across the plasma membrane via conformational changes, and ligand bias occurs when different ligands induce different types of conformational changes. For a long time, RTKs were believed to signal via a fundamentally different mechanism involving ligand-induced lateral dimerization. Recently it has become clear, however, that this simple model fails to capture all the complexities of RTK signaling and that the bound ligands need to induce conformational changes in RTK dimers for efficient downstream signaling to occur. Thus, both RTK dimer formation and conformational changes in the RTK dimer are required for RTK activation in the plasma membrane. Likewise, RTK ligand bias occurs due to both ligand-specific dimerization propensities and ligand-specific conformational changes.

4-4: References

[1] J. Schlessinger, "Cell signaling by receptor tyrosine kinases.," *Cell*, vol. 103, no. 2, pp. 211–25, Oct. 2000.

[2] M. A. Lemmon and J. Schlessinger, "Cell signaling by receptor tyrosine kinases.," *Cell*, vol. 141, no. 7, pp. 1117–34, Jun. 2010.

[3] W. J. Fantl, D. E. Johnson, and L. T. Williams, "Signalling by receptor tyrosine kinases.," *Annu. Rev. Biochem.*, vol. 62, pp. 453–81, 1993.

[4] A. A. Belov and M. Mohammadi, "Molecular mechanisms of fibroblast growth factor signaling in physiology and pathology.," *Cold Spring Harb. Perspect. Biol.*, vol. 5, no. 6, Jun. 2013.

[5] C. L. Arteaga and J. A. Engelman, "ERBB receptors: from oncogene discovery to basic science to mechanism-based cancer therapeutics.," *Cancer Cell*, vol. 25, no. 3, pp. 282–303, Mar. 2014.

[6] E. Ulupinar, M. F. Jacquin, and R. S. Erzurumlu, "Differential effects of NGF and NT-3 on embryonic trigeminal axon growth patterns.," *J. Comp. Neurol.*, vol. 425, no. 2, pp. 202–18, Sep. 2000.

[7] C. Hidai *et al.*, "FGF-1 enhanced cardiogenesis in differentiating embryonal carcinoma cell cultures, which was opposite to the effect of FGF-2.," *J. Mol. Cell. Cardiol.*, vol. 35, no. 4, pp. 421–5, Apr. 2003.

[8] R. Kuruvilla *et al.*, "A neurotrophin signaling cascade coordinates sympathetic neuron development through differential control of TrkA trafficking and retrograde signaling.," *Cell*, vol. 118, no. 2, pp. 243–55, Jul. 2004.

[9] M. C. Zaccaro *et al.*, "Selective small molecule peptidomimetic ligands of TrkC and TrkA

receptors afford discrete or complete neurotrophic activities.," *Chem. Biol.*, vol. 12, no. 9, pp. 1015–28, Sep. 2005.

[10] M. Jensen, B. Hansen, P. De Meyts, L. Schäffer, and B. Ursø, "Activation of the insulin receptor by insulin and a synthetic peptide leads to divergent metabolic and mitogenic signaling and responses.," *J. Biol. Chem.*, vol. 282, no. 48, pp. 35179–86, Nov. 2007.

[11] D. Chen *et al.*, "Bivalent peptidomimetic ligands of TrkC are biased agonists and selectively induce neuritogenesis or potentiate neurotrophin-3 trophic signals.," *ACS Chem. Biol.*, vol. 4, no. 9, pp. 769–81, Sep. 2009.

[12] K. J. Wilson, J. L. Gilmore, J. Foley, M. A. Lemmon, and D. J. Riese, "Functional selectivity of EGF family peptide growth factors: implications for cancer.," *Pharmacol. Ther.*, vol. 122, no. 1, pp. 1–8, Apr. 2009.

[13] L. Sciacca *et al.*, "Insulin analogues differently activate insulin receptor isoforms and post-receptor signalling.," *Diabetologia*, vol. 53, no. 8, pp. 1743–53, Aug. 2010.

[14] D. M. Freed *et al.*, "EGFR Ligands Differentially Stabilize Receptor Dimers to Specify Signaling Kinetics.," *Cell*, vol. 171, no. 3, p. 683–695.e18, Oct. 2017.

[15] C. Sweeney, C. Lai, D. J. Riese, A. J. Diamonti, L. C. Cantley, and K. L. Carraway, "Ligand discrimination in signaling through an ErbB4 receptor homodimer.," *J. Biol. Chem.*, vol. 275, no. 26, pp. 19803–7, Jun. 2000.

[16] C. Jørgensen *et al.*, "Cell-specific information processing in segregating populations of Eph receptor ephrin-expressing cells.," *Science*, vol. 326, no. 5959, pp. 1502–9, Dec. 2009.

[17] M. Barbacid, "The Trk family of neurotrophin receptors.," *J. Neurobiol.*, vol. 25, no. 11, pp. 1386–403, Nov. 1994.

[18] K. Ohira and M. Hayashi, “A new aspect of the TrkB signaling pathway in neural plasticity.,” *Curr. Neuropharmacol.*, vol. 7, no. 4, pp. 276–85, Dec. 2009.

[19] E. S. Levine, C. F. Dreyfus, I. B. Black, and M. R. Plummer, “Brain-derived neurotrophic factor rapidly enhances synaptic transmission in hippocampal neurons via postsynaptic tyrosine kinase receptors.,” *Proc. Natl. Acad. Sci. U. S. A.*, vol. 92, no. 17, pp. 8074–7, Aug. 1995.

[20] A. Figurov, L. D. Pozzo-Miller, P. Olafsson, T. Wang, and B. Lu, “Regulation of synaptic responses to high-frequency stimulation and LTP by neurotrophins in the hippocampus.,” *Nature*, vol. 381, no. 6584, pp. 706–9, Jun. 1996.

[21] W. Gottschalk, L. D. Pozzo-Miller, A. Figurov, and B. Lu, “Presynaptic modulation of synaptic transmission and plasticity by brain-derived neurotrophic factor in the developing hippocampus.,” *J. Neurosci.*, vol. 18, no. 17, pp. 6830–9, Sep. 1998.

[22] B. Xu *et al.*, “The role of brain-derived neurotrophic factor receptors in the mature hippocampus: modulation of long-term potentiation through a presynaptic mechanism involving TrkB.,” *J. Neurosci.*, vol. 20, no. 18, pp. 6888–97, Sep. 2000.

[23] Y. Kovalchuk, E. Hanse, K. W. Kafitz, and A. Konnerth, “Postsynaptic Induction of BDNF-Mediated Long-Term Potentiation.,” *Science*, vol. 295, no. 5560, pp. 1729–34, Mar. 2002.

[24] M. V Chao, “Neurotrophins and their receptors: a convergence point for many signalling pathways.,” *Nat. Rev. Neurosci.*, vol. 4, no. 4, pp. 299–309, Apr. 2003.

[25] C. R. Bramham and E. Messaoudi, “BDNF function in adult synaptic plasticity: the synaptic consolidation hypothesis.,” *Prog. Neurobiol.*, vol. 76, no. 2, pp. 99–125, Jun. 2005.

[26] R. Klein, L. F. Parada, F. Coulier, and M. Barbacid, “trkB, a novel tyrosine protein kinase receptor expressed during mouse neural development.,” *EMBO J.*, vol. 8, no. 12, pp. 3701–9, Dec. 1989.

[27] R. Klein, D. Conway, L. F. Parada, and M. Barbacid, “The trkB tyrosine protein kinase gene codes for a second neurogenic receptor that lacks the catalytic kinase domain.,” *Cell*, vol. 61, no. 4, pp. 647–56, May 1990.

[28] D. Soppet *et al.*, “The neurotrophic factors brain-derived neurotrophic factor and neurotrophin-3 are ligands for the trkB tyrosine kinase receptor.,” *Cell*, vol. 65, no. 5, pp. 895–903, May 1991.

[29] V. Wong, R. Arriaga, N. Y. Ip, and R. M. Lindsay, “The neurotrophins BDNF, NT-3 and NT-4/5, but not NGF, up-regulate the cholinergic phenotype of developing motor neurons.,” *Eur. J. Neurosci.*, vol. 5, no. 5, pp. 466–74, May 1993.

[30] H. Thoenen and Y. A. Barde, “Physiology of nerve growth factor.,” *Physiol. Rev.*, vol. 60, no. 4, pp. 1284–335, Oct. 1980.

[31] D. R. Kaplan and F. D. Miller, “Neurotrophin signal transduction in the nervous system.,” *Curr. Opin. Neurobiol.*, vol. 10, no. 3, pp. 381–91, Jun. 2000.

[32] J. Hall, K. L. Thomas, and B. J. Everitt, “Rapid and selective induction of BDNF expression in the hippocampus during contextual learning.,” *Nat. Neurosci.*, vol. 3, no. 6, pp. 533–5, Jun. 2000.

[33] C. C. Proenca, M. Song, and F. S. Lee, “Differential effects of BDNF and neurotrophin 4 (NT4) on endocytic sorting of TrkB receptors.,” *J. Neurochem.*, vol. 138, no. 3, pp. 397–406, 2016.

[34] M. V Chao, R. Rajagopal, and F. S. Lee, “Neurotrophin signalling in health and disease.,”

Clin. Sci. (Lond)., vol. 110, no. 2, pp. 167–73, Feb. 2006.

[35] S. L. Patterson, T. Abel, T. A. Deuel, K. C. Martin, J. C. Rose, and E. R. Kandel, "Recombinant BDNF rescues deficits in basal synaptic transmission and hippocampal LTP in BDNF knockout mice.," *Neuron*, vol. 16, no. 6, pp. 1137–45, Jun. 1996.

[36] A. L. Carvalho, M. V Caldeira, S. D. Santos, and C. B. Duarte, "Role of the brain-derived neurotrophic factor at glutamatergic synapses.," *Br. J. Pharmacol.*, vol. 153 Suppl, pp. S310-24, Mar. 2008.

[37] C. Lodovichi, N. Berardi, T. Pizzorusso, and L. Maffei, "Effects of neurotrophins on cortical plasticity: same or different?," *J. Neurosci.*, vol. 20, no. 6, pp. 2155–65, Mar. 2000.

[38] J. T. Erickson *et al.*, "Mice lacking brain-derived neurotrophic factor exhibit visceral sensory neuron losses distinct from mice lacking NT4 and display a severe developmental deficit in control of breathing.," *J. Neurosci.*, vol. 16, no. 17, pp. 5361–71, Sep. 1996.

[39] G. Fan *et al.*, "Knocking the NT4 gene into the BDNF locus rescues BDNF deficient mice and reveals distinct NT4 and BDNF activities.," *Nat. Neurosci.*, vol. 3, no. 4, pp. 350–7, Apr. 2000.

[40] N. Y. Ip *et al.*, "Mammalian neurotrophin-4: structure, chromosomal localization, tissue distribution, and receptor specificity.," *Proc. Natl. Acad. Sci. U. S. A.*, vol. 89, no. 7, pp. 3060–4, Apr. 1992.

[41] J. Philo, J. Talvenheimo, J. Wen, R. Rosenfeld, A. Welcher, and T. Arakawa, "Interactions of neurotrophin-3 (NT-3), brain-derived neurotrophic factor (BDNF), and the NT-3.BDNF heterodimer with the extracellular domains of the TrkB and TrkC receptors.," *J. Biol. Chem.*, vol. 269, no. 45, pp. 27840–6, Nov. 1994.

[42] M. J. Banfield, R. L. Naylor, A. G. Robertson, S. J. Allen, D. Dawbarn, and R. L. Brady, "Specificity in Trk receptor:neurotrophin interactions: the crystal structure of TrkB-d5 in complex with neurotrophin-4/5.," *Structure*, vol. 9, no. 12, pp. 1191–9, Dec. 2001.

[43] R. L. Naylor *et al.*, "A discrete domain of the human TrkB receptor defines the binding sites for BDNF and NT-4.," *Biochem. Biophys. Res. Commun.*, vol. 291, no. 3, pp. 501–7, Mar. 2002.

[44] C. King, S. Sarabipour, P. Byrne, D. J. Leahy, and K. Hristova, "The FRET signatures of noninteracting proteins in membranes: simulations and experiments.," *Biophys. J.*, vol. 106, no. 6, pp. 1309–17, Mar. 2014.

[45] C. King, V. Raicu, and K. Hristova, "Understanding the FRET Signatures of Interacting Membrane Proteins.," *J. Biol. Chem.*, vol. 292, no. 13, pp. 5291–5310, Mar. 2017.

[46] P. K. Wolber and B. S. Hudson, "An analytic solution to the Förster energy transfer problem in two dimensions.," *Biophys. J.*, vol. 28, no. 2, pp. 197–210, Nov. 1979.

[47] L. Chen, L. Novicky, M. Merzlyakov, T. Hristov, and K. Hristova, "Measuring the energetics of membrane protein dimerization in mammalian membranes.," *J. Am. Chem. Soc.*, vol. 132, no. 10, pp. 3628–35, Mar. 2010.

[48] T. A. Bowden *et al.*, "Structural Plasticity of Eph-Receptor A4 Facilitates Cross-Class Ephrin Signaling.," *Structure*, vol. 17, no. 12, p. 1679, Dec. 2009.

[49] C. Lu, L.-Z. Mi, T. Schürpf, T. Walz, and T. A. Springer, "Mechanisms for kinase-mediated dimerization of the epidermal growth factor receptor.," *J. Biol. Chem.*, vol. 287, no. 45, pp. 38244–53, Nov. 2012.

[50] N. F. Endres *et al.*, "Conformational coupling across the plasma membrane in activation of the EGF receptor.," *Cell*, vol. 152, no. 3, pp. 543–56, Jan. 2013.

[51] N. J. Bessman, D. M. Freed, and M. A. Lemmon, “Putting together structures of epidermal growth factor receptors.,” *Curr. Opin. Struct. Biol.*, vol. 29, pp. 95–101, Dec. 2014.

[52] E. V Bocharov *et al.*, “Helix-helix interactions in membrane domains of bitopic proteins: Specificity and role of lipid environment.,” *Biochim. Biophys. acta. Biomembr.*, vol. 1859, no. 4, pp. 561–576, Apr. 2017.

Chapter 5: Deciphering the mechanism behind hß-NGF and h-NT-3 functional selectivity

5-1: Introduction

We have shown that Trk-A signals via lateral dimerization in the plasma membrane, which brings the two catalytic domains in close proximity, allowing them to cross-phosphorylate each other (data for dimerization of Trk-A shown in Chapter 3). The studies of Trk-A dimerization and changes in dimer conformation upon cognate ligand binding, hß-NGF, have shown that Trk-A forms dimers in the absence of ligand, and that ligand binding to the Trk-A dimer stabilizes the dimer further and causes a change in the dimer conformation [1].

Trk-A signaling is crucial for the development of the nervous system. The functioning of the nervous system relies on the establishment of precise neuronal circuits through a developmental program including neuronal proliferation, axonal growth and guidance, target field innervation, neuronal survival and synaptogenesis [2][3][4][5][6][7][8]. The neurotrophic growth factors such as Nerve Growth Factor (hß-NGF) and Neurotrophin-3 (h-NT-3) have been shown to control diverse aspects of neuron development by interacting with Trk-A. However, a fundamental question is how the two different neurotrophins, h-NT-3 and hß-NGF, signal through the common Trk-A to coordinate distinct stages of sympathetic neuron development [9]. Previous research has shown that h-NT-3 signals through cell-surface Trk-A receptors to promote axon growth. In contrast, hß-NGF supports both axonal growth and neuronal survival through internalization and trafficking of hß-NGF: Trk-A-containing signaling endosomes back to the cell bodies to regulate changes in gene expression.

Ligand functional selectivity or ligand biased signaling is defined as the ability of

different ligands to activate distinct signaling pathways through a common receptor. It has been described for other ligand-RTK pairs [10][11]. Thus, this work will seek to decipher how Trk-A receptor-mediated specificity is achieved in response to two ligands. In chapter 4, we have shown that Trk-B interacts with three different ligands to generate diverse biological responses. In the case of Trk-B activation in response to Brain Derived Neurotrophic Factor (h-BDNF), Neurotrophin-3 (h-NT-3), and Neurotrophin-4 (h-NT-4), each neurotrophin induces a change in the conformation of transmembrane region of the Trk-B receptor, resulting in distinct kinase conformations. We have also found that the three ligands stabilize the TrkB dimers to different extents.

In this chapter we test our hypothesis that the distinct biological responses of Trk-A to its ligands correlate with different stabilities and/or different conformation of the Trk-A dimers elicited by each ligand. This study will allow us to determine whether Trk-A and B receptors, which are highly homologous in terms of their percent sequence identities, recognize different ligands using similar mechanism. This hypothesis will be tested by using the FRET-based method which yields both thermodynamic and structural information about RTK dimers as described in detail in chapter 2 [12][13][14].

5-2: Results

In chapter 3 we have measured the dimerization of Trk-A in the plasma membrane. To allow for FRET detection, the receptors were tagged with fluorescent proteins (either mTurquoise (mTurq) or YFP, a FRET pair) at their C-termini, attached via a $(GGS)_5$ flexible linkers. The cells were imaged with a spectrally resolved two-photon microscope and analyzed with a software package developed in the lab to obtain (i) the donor concentrations, (ii) the acceptor concentrations, and, (iii) the FRET efficiencies, in live cells. A model describing the monomer-dimer equilibrium was used to fit the data, yielding dimerization curves and dissociation constants that describe the stabilities of the dimers.

Dimerization curves were first acquired for Trk-A in the absence of ligand as shown in chapter 3 in figure 3-1, yielding a two-dimensional dimer dissociation constant of 132 ± 37 receptors/μm^2. Then, experiments were performed with Trk-A in the presence of saturating ligand concentration (380 nM) of h-NT-3 and hß-NGF. Data are shown in figures 5-1-A and 5-1-C, respectively. This concentration greatly exceeds the dissociation constant for h-NT-3-Trk-A and hß-NGF binding (1 nM), and ensures that all Trk-A dimers are bound to h-NT-3 and hß-NGF. The solid line in black in figure 5-1-A and 5-1-C represents "proximity" FRET and it is accounted for in figure 5-1-E to obtain FRET that occurs due to specific interaction between Trk-A receptor in the presence of ligands. Figure 5-1-E shows the corrected FRET as a function of total receptor concentration. We see that the corrected FRET is not concentration dependent, suggesting that Trk-A is dimeric over a broad range of concentrations in our experiment when treated with these ligands. The binned dimeric fractions in the presence of both ligands are shown in figure 5-1-G.

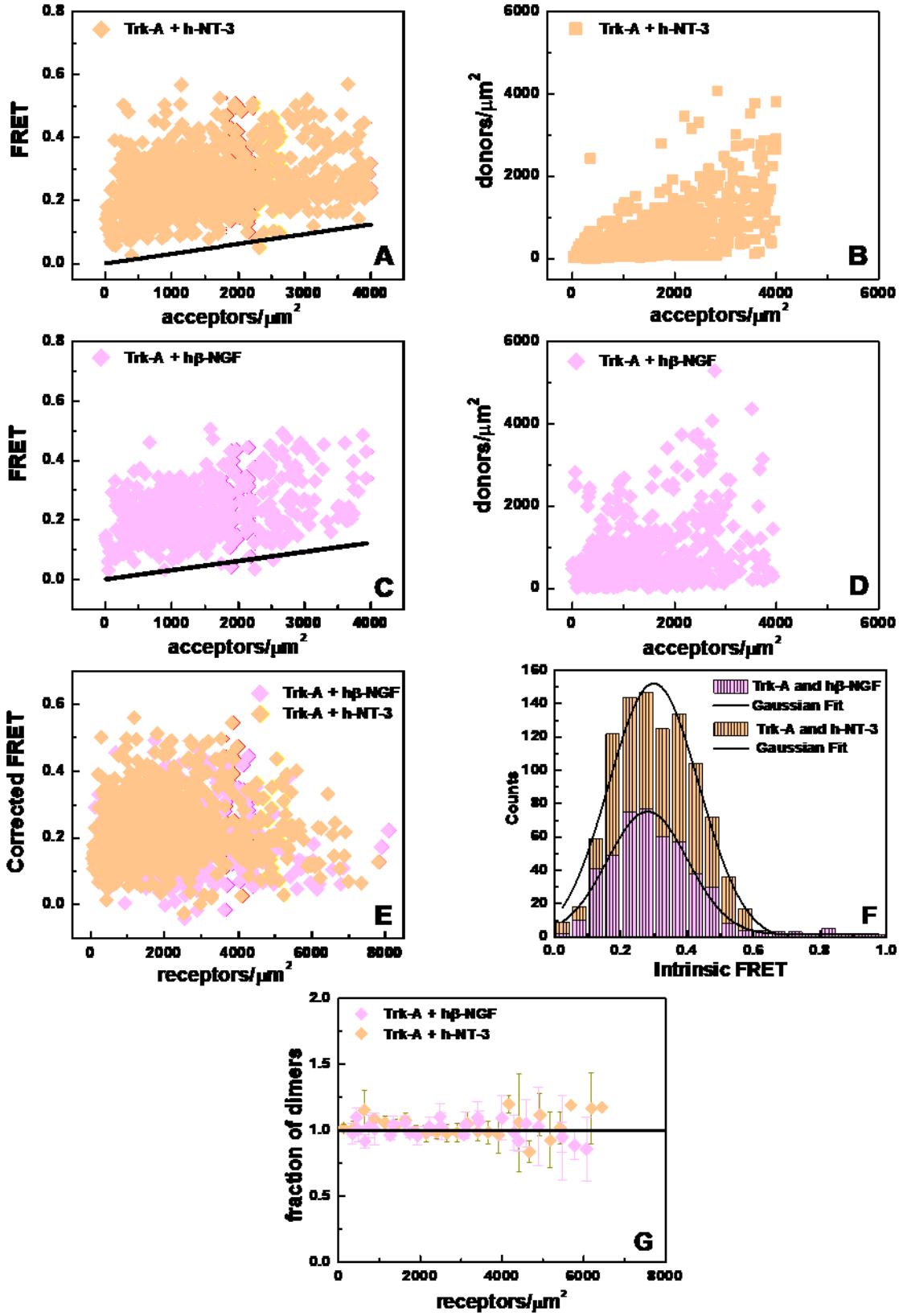
Trk-A + h-NT-3
FRET
acceptors/μm²
A
donors/μm²
B
Trk-A + hβ-NGF
C
D
Corrected FRET
receptors/μm²
E
Trk-A and hβ-NGF
Gaussian Fit
Trk-A and h-NT-3
Counts
Intrinsic FRET
F
fraction of dimers
G

Figure 5- 1: Comparison of the FRET data for full length Trk-A in the presence of saturating concentrations of h-NT-3 and hß-NGF. A and C: the FRET data plotted as a function of acceptor concentration for Trk-A in the presence of h-NT-3 and hß-NGF. Black straight line in the graph represents the "proximity" FRET. B and D: donor concentration and acceptor concentration for full length Trk-A in the presence of the two ligands. E, corrected FRET plotted as a function of total receptor concentration. F: histograms and Gaussian fits of FRET data for h-NT-3 and hß-NGF. G, fraction of dimers as a function of total receptor concentration for Trk-A in the presence of h-NT-3 and hß-NGF. The dimerization parameters obtained from this data are reported in Table 5-1.

Constructs	K_{diss} (rec/μm²)	ΔG (kcal/mol)	Intrinsic FRET (Ẽ)	d(Å)
Trk-A+NGF	100% dimer	n.d.[a]	0.28 ± 0.02	64 ± 1
Trk-A+NT-3	100% dimer	n.d.[a]	0.29 ± 0.02 n.s.	63 ± 1

Table 5- 1: Dimerization parameters for full length Trk-A in the presence of h-NT-3 and hß-NGF. (a- n.d. not determined, n.s. not statistically significant as determined by ANOVA-test).

The dimer stability of the h-NT-3 and hß-NGF-bound full length Trk-A dimers is very high, such that only 100% dimers are present at all Trk-A concentrations in the experiments as shown in figure 5-1-G. These results suggest that Trk-A forms stable dimers in the presence of both ligands. The Trk-A two-dimensional dissociation constant is therefore < 5 receptors/μm^2 in the presence of these ligands, the experimental cut-off. To obtain information regarding Intrinsic FRET, we used equation 11 (since the dimeric fraction is 1). The data is plotted as histograms and was fitted with Gaussian functions to determine the mean and standard errors, shown in Table 5-1. The means give information regarding the average positioning of the fluorophores attached to the Trk-A receptor. There are no significant differences between the Intrinsic FRET values reported in Table 5-1, indicating that the two ligands stabilize similar conformations of the Trk-A dimer that are indistinguishable in our experiments.

The FRET data for ECTM-Trk-A, with a kinase domain that has been removed as described in Chapter 2, in the presence of h-NT-3 and hß-NGF is shown in Figure 5-2. ECTM-Trk-A was treated with saturating concentration of ligands (380nM). Figures 5-2-A and C show FRET as a function of acceptor concentration in the presence of h-NT-3 and hß-NGF, respectively. The solid black line in these plots represents the contribution due to proximity FRET. Figures 5-2-B and 5-2-D show the donor concentration versus the acceptor concentration for Trk-A in the presence of h-NT-3 and hß-NGF. The corrected FRET efficiency, which is due to specific interaction between ECTM-Trk-A receptors, is plotted as a function of total receptor concentration. As we can see, in figure 5-2-E, the specific FRET increases as a function of the concentration of the receptor. This indicates that the concentration of dimer increases, according to the law of mass action. A monomer-dimer equilibrium model was fitted to the corrected FRET data as shown in figure 5-2-F. This fit yields two parameters: the dissociation constant, K, which reports on the strength of

ECTM-Trk-A interaction, and the Intrinsic FRET, a structural parameter. These values are reported in Table 5-2. Experimental binned fractions of dimers as a function of total receptors in the presence of the two ligands is shown in figure 5-2-F, along with the best fit solid line.

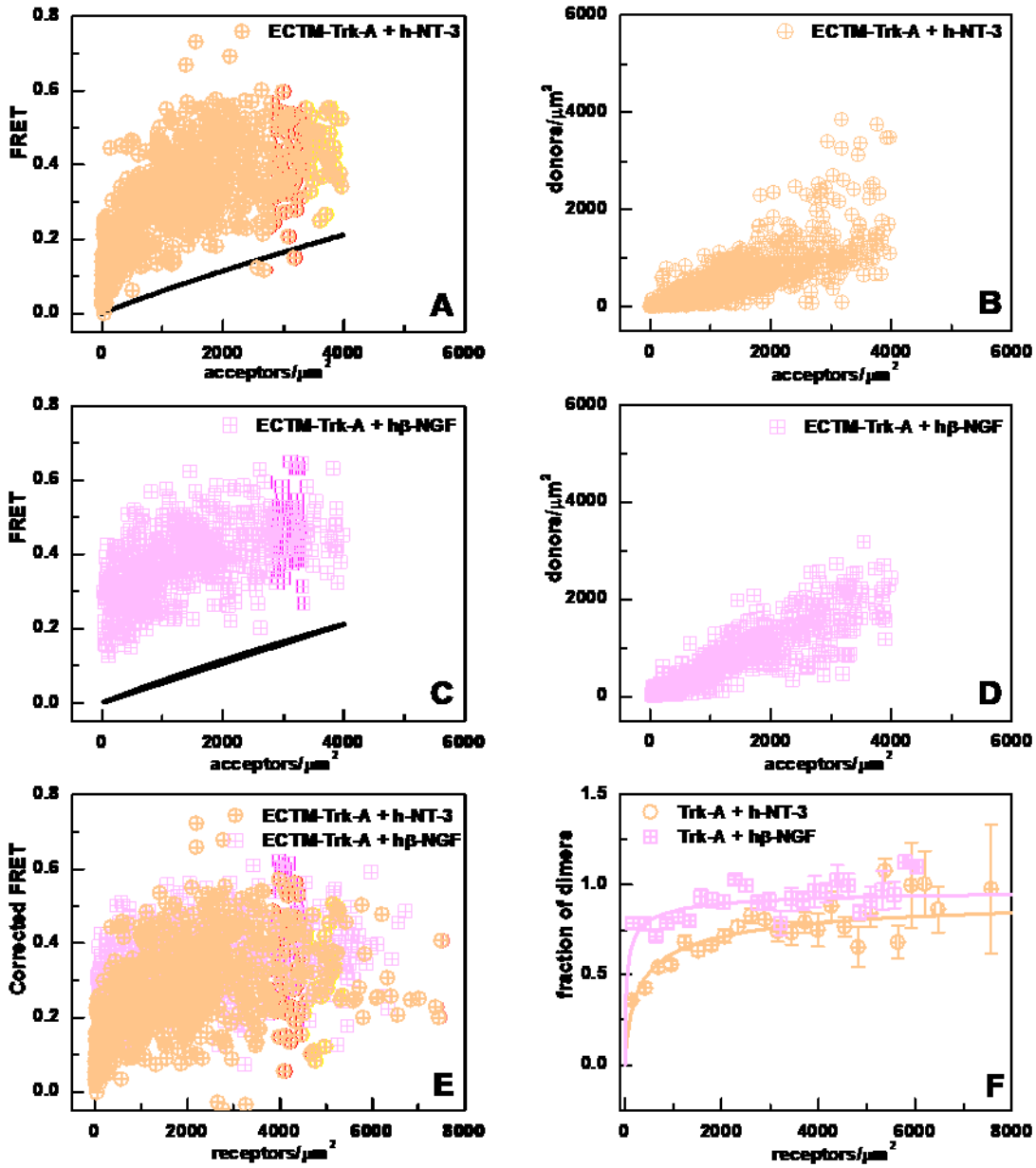

Figure 5- 2: ECTM-Trk-A FRET data in the presence of h-NT-3 and hß-NGF is being compared. A and C: FRET as a function of acceptor concentration for h-NT-3 and hß-NGF. The black solid line indicates the "proximity" FRET. B and D: ECTM-Trk-A donor vs. acceptor plot for the two ligands. E: corrected FRET as a function of total receptor concentration. F: the dimerization curves for ECTM-TRK-A in the presence of hß-NGF and h-NT-3. The measured dimeric

fractions are binned and are shown with symbols, along with the standard errors. The solid line is the best fit for a monomer-dimer equilibrium model.

Constructs	K_{diss} (rec/μm²)	ΔG (kcal/mol)	Intrinsic FRET (Ẽ)	d(Å)
ECTM-Trk-A + h-NT-3	456±75	-4.56±0.10 ****	0.61±0.02 n.s.	50 ± 1
ECTM-Trk-A+ hß-NGF	25 ± 5	-6.28 ± 0.12	0.59 ± 0.01	51 ± 1

Table 5- 2: Dimerization parameters for ECTM-Trk-A in the presence of h-NT-3 and hß-NGF (**** p-value is < 0.0001; n.s. not statistically significant as determined by ANOVA-test).

As shown in figure 5-2-F, Trk-A dimer stability in the presence of h-NT-3 is much lower, when compared to the hß-NGF case. The two-dimensional dissociation constant for h-NT3 is 456±75 rec/μm^2 and for hß-NGF is 25 ± 5 rec/μm^2 (Table 5-2). Yet, virtually all Trk-A receptors in these experiments are ligand-bound at this very high ligand concentration. This shows that Trk-A in the presence of the two different ligands exhibits statistically significant differences in dimer stability in the plasma membrane. Unlike in the case of Trk-B described in chapter 4, we were not able to detect a difference in Intrinsic FRET, and therefore in the conformation of Trk-A dimer, in the presence of these two ligands.

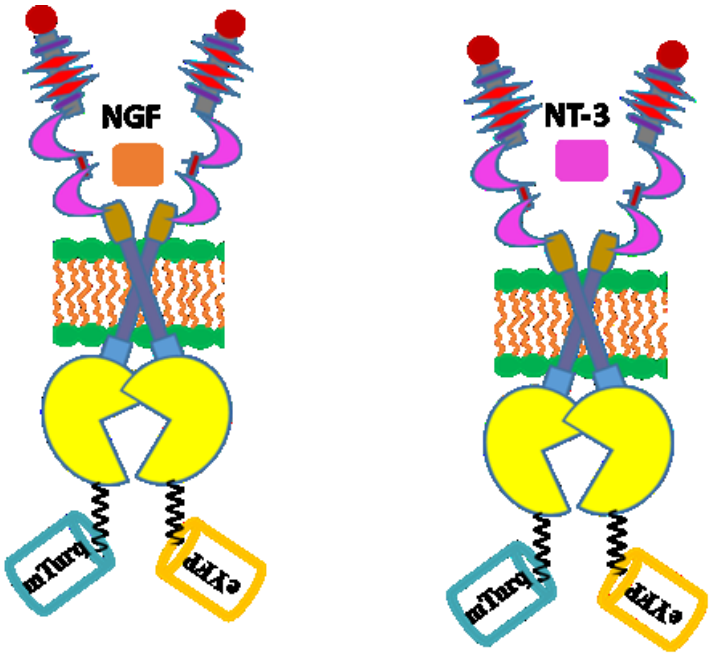

Figure 5- 3: A cartoon of Trk-A in the presence of h-NT-3 and hß-NGF, depicting no measurable differences in the fluorescent protein positioning when the two ligands are bound to the EC domain. Instead we see differences in dimer stability for the Trk-A receptor for the two ligands as reported in Table 5-1 and 5-2.

As shown in figure 5-3 and table 5-2, the only change was observed in the stability of the dimer, specific to each ligand.

5-3: Discussion

How multiple neurotrophins can interact with the same receptor to generate distinct biological response in neuronal cells is still largely unknown. Here we investigated how information is transmitted via the Trk-A receptor when two different neurotrophins interact with the receptor at the plasma membrane to produce different biological responses. We have previously shown in chapter 4 that Trk-B interacts with three different ligands, and each ligand is responsible for causing different conformational change and having different effects on the stability of Trk-B dimer.

We did similar experiments to investigate how two different ligands, h-NT-3 and hß-NGF, can interact with Trk-A in the plasma membrane. To determine the stability effects of h-NT-3 and hß-NGF bound ligand, we measured and compared the thermodynamic stability of the Trk-A dimer in the presence of saturating concentrations of these ligands. We also measured and compared the Intrinsic FRET for Trk-A in the presence of saturating concentrations of h-NT-3 and hß-NGF to determine any conformation differences in the Trk-A dimer.

As mentioned in the introduction section, hß-NGF, but not h-NT-3, results in endocytosis and retrograde trafficking of Trk-A receptors from axon terminals back to neuronal cell bodies to activate transcriptional programs necessary for sympathetic neuron survival. Conversely, local h-NT-3-TrkA signaling in axons is sufficient to promote axon growth. This intriguing difference between the actions of h-NT-3 and hß-NGF observed in the biology of neuronal cells is due to the ligand biased signaling which gets initiated at the plasma membrane level. We have shown that h-NT-3-induced Trk-A dimers are less stable compared to hß-NGF-induced receptor dimers

(Figure 5-2, Table 5-2). However, we were not able to detect differences in the conformation of Trk-A dimer in the presence of the for two ligands (Figure 5-3, Table 5-1 and 5-2). Differences may exist, but they may be too subtle to be captured with the FRET assay.

Together, this analysis suggests that Trk-A dimer stability correlates with distinct biological outcomes, i.e. stable dimers promote neuron survival and growth and weaker dimers promote axon growth, but not neuron survival. This new knowledge will enhance our understanding of the development of the nervous system, and will open the door for novel ways to control neuronal growth. We can engineer ligands that may stabilize the Trk-A dimer to a different extent, and these may induce new types of neuronal responses, which significantly differ from the ones found in nature.

5-4: References

[1] F. Ahmed and K. Hristova, “Dimerization of the Trk receptors in the plasma membrane: effects of their cognate ligands.,” *Biochem. J.*, vol. 475, no. 22, pp. 3669–3685, Nov. 2018.

[2] M. Bibel and Y. A. Barde, “Neurotrophins: key regulators of cell fate and cell shape in the vertebrate nervous system.,” *Genes Dev.*, vol. 14, no. 23, pp. 2919–37, Dec. 2000.

[3] G. M. Brodeur *et al.*, “Trk receptor expression and inhibition in neuroblastomas.,” *Clin. Cancer Res.*, vol. 15, no. 10, pp. 3244–50, May 2009.

[4] J. R. Chan, J. M. Cosgaya, Y. J. Wu, and E. M. Shooter, “Neurotrophins are key mediators of the myelination program in the peripheral nervous system.,” *Proc. Natl. Acad. Sci. U. S. A.*, vol. 98, no. 25, pp. 14661–8, Dec. 2001.

[5] B. L. Hempstead and J. L. Salzer, “Neurobiology. A glial spin on neurotrophins.,” *Science*, vol. 298, no. 5596, pp. 1184–6, Nov. 2002.

[6] A. Patapoutian and L. F. Reichardt, “Trk receptors: mediators of neurotrophin action.,” *Curr. Opin. Neurobiol.*, vol. 11, no. 3, pp. 272–80, Jun. 2001.

[7] M. V Sofroniew, C. L. Howe, and W. C. Mobley, “Nerve growth factor signaling, neuroprotection, and neural repair.,” *Annu. Rev. Neurosci.*, vol. 24, pp. 1217–81, 2001.

[8] F. D. Miller and D. R. Kaplan, “Neurobiology. TRK makes the retrograde.,” *Science*, vol. 295, no. 5559, pp. 1471–3, Feb. 2002.

[9] R. Kuruvilla *et al.*, “A neurotrophin signaling cascade coordinates sympathetic neuron development through differential control of TrkA trafficking and retrograde signaling.,”

Cell, vol. 118, no. 2, pp. 243–55, Jul. 2004.

[10] K. J. Wilson, J. L. Gilmore, J. Foley, M. A. Lemmon, and D. J. Riese, "Functional selectivity of EGF family peptide growth factors: implications for cancer.," *Pharmacol. Ther.*, vol. 122, no. 1, pp. 1–8, Apr. 2009.

[11] F. V Mariani, C. P. Ahn, and G. R. Martin, "Genetic evidence that FGFs have an instructive role in limb proximal-distal patterning.," *Nature*, vol. 453, no. 7193, pp. 401–5, May 2008.

[12] L. Chen, L. Novicky, M. Merzlyakov, T. Hristov, and K. Hristova, "Measuring the energetics of membrane protein dimerization in mammalian membranes.," *J. Am. Chem. Soc.*, vol. 132, no. 10, pp. 3628–35, Mar. 2010.

[13] S. Sarabipour, N. Del Piccolo, and K. Hristova, "Characterization of membrane protein interactions in plasma membrane derived vesicles with quantitative imaging Förster resonance energy transfer.," *Acc. Chem. Res.*, vol. 48, no. 8, pp. 2262–9, Aug. 2015.

[14] C. King, M. Stoneman, V. Raicu, and K. Hristova, "Fully quantified spectral imaging reveals in vivo membrane protein interactions.," *Integr. Biol. (Camb).*, vol. 8, no. 2, pp. 216–29, Feb. 2016.

Chapter 6: Conclusions

Despite decades of Receptor Tyrosine Kinase (RTK) research, the mechanism of RTK activation in response to their ligands is still under debate. Receptor tyrosine kinases (RTKs) are cell surface receptors, which control cell growth and differentiation, and play important roles in tumorigenesis. The main goal of my research was to study the interactions that control the activation of the Tropomyosin receptor kinase (Trk) family of RTKs in the plasma membrane, using a FRET-based methodology. The Trk receptors are expressed in neuronal tissues, and they guide the development of the central and peripheral nervous systems during development. We quantified the dimerization of human Trk-A, Trk-B, and Trk-C in the absence and presence of their cognate ligands: human ß-nerve growth factor (hß-NGF), human brain-derived neurotrophic factor (h-BDNF), and human neurotrophin-3 (h-NT-3), respectively. We have also assessed conformational changes in the Trk dimers upon ligand binding. A crosslinking assay was performed for Trk-A in the absence and presence of hß-NGF to determine its oligomer state. We also investigated how one receptor can respond to multiple ligands to generate ligand biased signaling for Trk-B and Trk-C.

In chapter 3, we have shown that our data support a model of Trk activation in which (1) Trks have a propensity to interact laterally and to form dimers even in the absence of ligand, (2) different Trk unliganded dimers have different stabilities, (3) ligand binding leads to Trk dimer stabilization and (4) ligand binding induces structural changes in the Trk dimers which propagate to their transmembrane and intracellular domains. This model, which we call the "transition model of RTK activation," may hold true for many other RTKs.

In chapter 4 and 5, ligand biased signaling was studied for Trk-A and Trk-B in the presence of additional ligands. Trk-B is known to interact with three different neurotrophins: Human Brain-

Derived Neurotrophic Factor (h-BDNF), human Neurotrophin-4 (h-NT-4) and human Neurotrophin-3 (h-NT-3). All three neurotrophins are involved in survival and proliferation of neuronal cells, but each one initiates different downstream biological response. Our results show that the Trk-B dimers, when bound to the different ligands, have different dimer stabilities and different conformations. Trk-A function is differentially controlled by hß-NGF and h-NT-3. For Trk-A, we observed differences in the stabilities of the Trk-A dimers that are bound to hß-NGF or h-NT-3, but we could not identify differences in dimer conformations using the FRET assay. The differences in stability or conformation of the different-ligand bound Trk dimers may be responsible for ligand biased signaling and for generating different biological responses. This new knowledge about Trk activation and ligand functional selectivity can be used to design new Trk modulators, for the benefit of human health.

Biographical Sketch

Fozia Ahmed was born on the 16th of August 1988 in Gujrat, Pakistan. She completed her high school education in Pakistan, and moved to USA for higher education. She obtained her bachelors of sciences from Denison University, Ohio, in 2010. During her undergraduate program she was exposed to research opportunities in the fields of Analytical Chemistry and Biochemistry. She went on pursuing a Master's of Biotechnology degree from Johns Hopkins University, with concentration in Molecular Targets and Drug Discovery technologies. She joined a prostate cancer focused research lab during her Master's and studied the role of microRNAs in silencing the expression of proteins involved in advancing prostate cancer. She found cancer research fascinating, and was inspired to join Professor Kalina Hristova's lab at Johns Hopkins University to pursue a Ph.D. in Materials Science and Engineering after obtaining her Master's degree.

Professor Hristova's lab studies membrane proteins, specifically, Receptor Tyrosine Kinases (RTKs) in live cells. Fozia chose one subclass of RTKs, Tropomyosin Receptor Kinases (Trks) for her dissertation research. She characterized the interaction of all three Trk receptors by using FRET-based methods. She utilized biological and engineering techniques to understand Trks interactions in the absence and presence of different ligands, and the conformational changes that occur in the Trk dimers in response to ligand binding. Besides her research, she also likes to cook, travel, and watch documentaries.